

UNCLASSIFIED

Copy
RM E50F02

6

NACA RM E50F02

~~17/7/50~~
c.2

110 15 1950

NACA

RESEARCH MEMORANDUM

EXTENSION OF BOUNDARY-LAYER HEAT-TRANSFER THEORY TO
COOLED TURBINE BLADES

By W. Byron Brown and Patrick L. Donoughe

Lewis Flight Propulsion Laboratory
Cleveland, Ohio

CLASSIFICATION CANCELLED

Author: J. W. Crowley Date: 12/11/53

EO 11501

By: MDA 1/2/54 See NACA CLASSIFIED DOCUMENT

R71867

This document contains classified information affecting the National Defense of the United States within the meaning of the Espionage Act, USC 5031 and 5041. Its transmission or the revelation of its contents in any manner to an unauthorized person is prohibited by law. Information so classified may be imparted only to persons in the military and naval services of the United States, appropriate civilian officers and employees of the Federal Government who have a legitimate interest therein, and to United States citizens of known loyalty and discretion who of necessity must be informed thereof.

NACA LIBRARY
CENTRAL LABORATORY

NATIONAL ADVISORY COMMITTEE FOR AERONAUTICS

WASHINGTON
August 11, 1950

UNCLASSIFIED



UNCLASSIFIED

NATIONAL ADVISORY COMMITTEE FOR AERONAUTICS

RESEARCH MEMORANDUMEXTENSION OF BOUNDARY-LAYER HEAT-TRANSFER THEORY TO
COOLED TURBINE BLADES

By W. Byron Brown and Patrick L. Donoughe

SUMMARY

A review of existing boundary-layer heat-transfer theory applicable to outside heat-transfer coefficients was made. The influences of Mach number, temperature ratio, and exponents of gas-property temperature relations were computed and were shown to be relatively small, when the gas is air, for Mach numbers less than 2 with temperature ratios between 1 and 4. An equation for the average heat transfer of a surface was derived for constant wall temperature when the boundary layer changed from laminar to turbulent on the surface. These results indicated that the parameters needed to calculate the Nusselt number are the Reynolds and Euler numbers and the transition ratio (length of surface with laminar boundary layer divided by total length of surface). Good agreement between the average heat transfer predicted by the theory and some experimental results from cylinders, an airfoil, and turbine blades was obtained.

INTRODUCTION

No satisfactory correlation of heat transfer from turbine blades is possible between cooled turbine blades of the impulse and the reaction type when the correlation schemes used for boiler pipes, heat exchangers, and reciprocating engines are applied. It is known that the convective heat-transfer rates between the fluids and the metals involved are dependent on the boundary layers. In the general case of heat transfer through the boundary layer, the stream temperature may differ appreciably from the wall or surface temperature, so that variations of specific heat, density, viscosity, and thermal conductivity should be considered, as well as the effects of Mach number and pressure gradient in the direction of flow.

Theoretical studies have been made of heat transfer through laminar and turbulent boundary layers of certain simple types. One of the earliest laminar studies was made by Pohlhausen (reference 1), who assumed no pressure gradient (flat plate), various Prandtl num-

UNCLASSIFIED

bers, and constant fluid properties through the boundary layer. This analysis was extended to include large Mach numbers (supersonic flow) and temperature ratios (the absolute temperature of the fluid outside the boundary layer divided by the absolute temperature of the wall) widely different from unity (references 2 to 4). Variations in specific heat and the temperature-viscosity law are also considered in reference 4. In references 5 and 6, the pressure gradient along the flow path is included, but constant fluid properties are assumed, thus implying temperature ratios near 1. All these analyses assume a constant wall temperature. Reference 7 considers variations in the wall temperature without a pressure gradient in the flow direction.

In the case of theoretical formulas for turbulent boundary layers, Reynolds analogy is usually employed. Summaries of the resulting formulas for heat transfer are given in references 8 and 9. The problem for incompressible flow in a pipe and over a flat plate is discussed in reference 10.

Some experimental results have been published on average outside heat-transfer rates between the gas and the turbine blades from stationary cascades. No nozzles preceded these cascades. Data on impulse blades with temperature ratios of 0.8 and 0.9 are given in references 11 and 12, respectively, and reference 13 gives results for temperature ratios above 1. Even though these results are plotted in the same manner, different correlations are shown for different cascades (reference 14). In order to unify such results, theoretical studies are needed and new parameters not used in tube investigations may be necessary.

The theoretical effects of the various parameters on the heat transfer with a laminar boundary layer and constant wall temperature were analyzed at the NACA Lewis laboratory and are discussed herein. With the assumptions of constant wall temperature and Mach numbers less than 2, a formula is derived for the average outside heat-transfer coefficient at points where the boundary layer is partly laminar and partly turbulent. The effect of two additional parameters, the Euler number and the transition ratio, are calculated and presented. Results from experimental investigations are assembled and compared with results calculated by means of the theoretical formulas.

STATUS OF BOUNDARY-LAYER THEORY WITH HEAT TRANSFER

1.346

When a fluid flows along a solid boundary, the part in immediate contact with the surface has zero velocity relative to the solid (reference 15, pp. 676-680); whereas in the free stream, the fluid has its greatest velocity relative to the solid. Between the wall and the free stream, the velocity changes continuously from zero to the free-stream value; this region is called the boundary layer. One of the characteristic features of this region is that it is very thin compared with the length of the body for the ranges of Reynolds numbers considered herein ($10^4 < Re < 10^6$). Under these circumstances (thin boundary layer), the same equations hold for curved surfaces as for plane ones for a laminar boundary layer (reference 15, p. 120), so that the radius of curvature will not enter into the solution in general (the stagnation point is an exception). Such a boundary layer is shown in figure 1, which greatly exaggerates the relative thickness of the boundary layer. The solid surface is shown in the figure as a plate placed in the middle of a converging channel and therefore subject to a decreasing pressure gradient for subsonic flow. The distance x is measured along the surface from the stagnation point and the y direction is perpendicular to the surface. (All symbols used in the report are defined in Appendix A.)

Equation for Heat-Transfer Coefficient

At the wall surface, heat leaves the fluid by conduction at the rate per unit time per unit area $k_w(\partial T/\partial y)_w$, where k_w is the thermal conductivity of the fluid at the wall temperature and $(\partial T/\partial y)_w$ is the temperature gradient perpendicular to the wall at the wall. This rate of conduction is equal to the amount of heat that enters the wall per unit time per unit area, usually given as the product of a heat-transfer coefficient H and a temperature difference between the fluid in the main stream and the wall. When the fluid is moving rapidly, an effective temperature T_e is used in the heat-transfer equation. Thus

$$H(T_e - T_w) = k_w \left(\frac{\partial T}{\partial y} \right)_w \quad (1)$$

where T_w is not a function of x .

The effective temperature T_e is not the temperature indicated by a thermometer moving with the fluid, nor is it the stagnation temperature indicated by a thermometer placed in a calming chamber where the fluid is brought to rest without heat transfer; that is, adiabatically. It is instead the temperature that satisfies equation (1) at a specific point x when $(\partial T/\partial y)_w$ approaches zero and H remains constant. Thus, $T_e = T_w$ in this case and, consequently, T_e is often called the adiabatic wall temperature. By utilizing this concept for the effective gas temperature, the differential equations of the boundary layer can be solved for $(\partial T/\partial y)_w$ and T_e , and H may be computed through the use of equation (1).

1346

Equations of Laminar Boundary Layer

The equations of the compressible laminar boundary layer for steady-state flow of an actual gas with heat transfer are (reference 4):

Momentum equation,

$$\rho u \frac{\partial u}{\partial x} + \rho v \frac{\partial u}{\partial y} = \frac{\partial}{\partial y} \left(\mu \frac{\partial u}{\partial y} \right) - \frac{\partial p}{\partial x} \quad (2)$$

Continuity equation,

$$\frac{\partial}{\partial x} (\rho u) + \frac{\partial}{\partial y} (\rho v) = 0 \quad (3)$$

Energy equation,

$$Jc_p \left(\rho u \frac{\partial T}{\partial x} + \rho v \frac{\partial T}{\partial y} \right) = \frac{\partial}{\partial y} \left(k \frac{\partial T}{\partial y} \right) + \mu \left(\frac{\partial u}{\partial y} \right)^2 + u \frac{\partial p}{\partial x} \quad (4)$$

In order to find the quantities $(\partial T/\partial y)_w$ and T_e shown in equation (1), two independent solutions of the boundary-layer equations are necessary. The first solution is for $(\partial T/\partial y)_w$ with the assumption that T_w is independent of x and with the following boundary conditions:

When

$$y = 0,$$

$$u = 0 = v$$

and

$$T = T_w = \text{constant}$$

and when

$$y = \delta,$$

$$u = U$$

and

$$T = T_\delta$$

The second solution is for T_e with the assumption that $(\partial T / \partial y)_w = 0$ and $T_e = T_w$, which is an unknown quantity to be determined by solving the boundary-layer equations.

Dimensionless Parameters

The solution of equations (1) to (4) will involve the quantities u , v , x , y , ρ , μ , c_p , k , T , p , H , U , ω , φ , and β . The quantities ω , φ , and β are exponents of the temperature relations of viscosity, thermal conductivity, and specific heat, respectively. When the equations are put into dimensionless form and solved, the previously mentioned physical quantities appear as a group of dimensionless parameters, so that the solution can be expressed in the form

$$\Psi(Nu, Re, Pr, M, Eu, T_x, \Lambda, \omega, \varphi, \beta) = 0 \quad (5)$$

where

$$Nu = \frac{hx}{k_w} = \text{Nusselt number}$$

$$Re = \frac{U \rho_w x}{\mu_w} = \text{Reynolds number}$$

$$Pr = \frac{c_{p,w} \mu_w}{k_w} = \text{Prandtl number}$$

$$M = \frac{U}{a} = \text{Mach number}$$

$$Eu = \frac{-\frac{\partial p}{\partial x}}{\rho_\delta U^2} = \text{Euler number}$$

$$T_r = \frac{T_\delta}{T_w} = \text{temperature ratio}$$

$$\Lambda = \frac{T_e - T_\delta}{U^2 / 2gJc_p} = \text{recovery factor}$$

$$\frac{\mu}{\mu_w} = \left(\frac{T}{T_w} \right)^\omega$$

$$\frac{k}{k_w} = \left(\frac{T}{T_w} \right)^\varphi$$

$$\frac{c_p}{c_{p,w}} = \left(\frac{T}{T_w} \right)^\beta$$

(6)

The Nusselt number h_x/k_w is a well-known heat-transfer parameter that can be derived from equation (1) by rearranging and multiplying both sides of the equation by the reference length x , thereby making equation (1) nondimensional.

The Reynolds number $U_0 x/\mu_w$ is a well-known parameter for fluid-flow problems relating the inertia to the viscous forces.

The Prandtl number $c_{p,w}\mu_w/k_w$ results from making equation (4) nondimensional and depends entirely upon the properties of the fluid.

The Mach number U/a and the temperature ratio T_δ/T_w appear in the solution when the heat generated in the boundary layer is not negligible and when large temperature differences, producing changes in property values, exist between the fluid and the body.

The Euler number $-\frac{\partial p/\partial x}{\rho_\delta U^2/x}$ is not as familiar a grouping as the preceding numbers. It measures the pressure gradient in a nondimensional fashion. Although the symbol for Euler number has appeared as m in previous boundary-layer investigations (references 5, 6, and 9), the symbol Eu is used in this report to conform to the notation for other dimensionless quantities, such as Re , Pr , and Nu . When the velocity varies as x^{Eu} , the partial differentials in the numerator become total differentials and the Euler number reduces to the constant value Eu , as shown in references 5 and 6.

The quantity T_e is often related to T_δ by the equation

$$T_e = T_\delta + \Lambda \frac{U^2}{2gJc_p} \quad (7)$$

where Λ is a dimensionless number called the recovery factor.

If large temperature differences exist between the gas and the solid surface, many of the physical quantities in the equations (c_p , μ , ρ , and k) vary by large amounts in the boundary layer. In figure 2, the values of μ , k , and c_p are plotted in a logarithmic scale against absolute temperature. The large variations may not result in large changes in the Nusselt number because some of these variations may be compensatory. These curves can be

closely approximated by straight lines on a logarithmic plot for moderate ranges of temperature, so that it is possible to write

$$\left. \begin{aligned} \mu/\mu_w &= (T/T_w)^\omega \\ k/k_w &= (T/T_w)^\phi \\ c_p/c_{p,w} &= (T/T_w)^\beta \end{aligned} \right\} (8)$$

where ω , ϕ , and β are exponents that will appear in equations (2) to (4) when the preceding substitutions are made for μ , k , and c_p . The usual substitution for ρ is made; that is, ρ varies inversely as the temperature and directly as the pressure. In the solution, the values of ω , ϕ , and β have an influence on the results when T_r is markedly different from 1.

Effect of Variation of Dimensionless Parameters on Nusselt Number for Laminar Boundary Layer

When solved for Nu , equation (5) takes the form

$$Nu = \psi_1 (Re, Pr, M, Eu, T_r, \omega, \phi, \beta) \quad (9)$$

and

$$\Lambda = \psi_2 (Pr, M, Eu, \omega, \phi, \beta) \quad (10)$$

The evaluation of the functions ψ_1 and ψ_2 presents a formidable mathematical problem. The NACA Lewis laboratory is now working out a numerical solution for the general case, where the gas properties in the boundary layer vary with the temperature and large pressure gradients are present in the free stream at the same time. Calculations have already been made by several investigators and in this paper for some simplified cases by which the first-order effects of the parameters, acting independently, can be determined. The effects on the Nusselt number of the other nondimensional numbers in equation (9) follow.

Effect of Reynolds number Re. - All the references dealing with heat transfer through a laminar boundary layer (references 1 to 9 and 15), no matter which of the other parameters are included or omitted, agree that Nu should be proportional to the square root of the Reynolds number (for example, reference 15, pp. 626-636). Thus,

$$Nu \propto \sqrt{Re} \quad (11)$$

Effect of Prandtl number Pr. - A simple and exact relation for the effect of the Prandtl number on the Nusselt number is impossible because of the way Pr enters into equation (4) when the equation is made nondimensional. The effect has been calculated (reference 15, pp. 624 and 626) in the case where $M \approx 0$, $T_r \approx 1$, and variations in c_p are not considered; that is, $\beta = 0$. It has been found that with $Eu = 0$ for $0.7 \leq Pr \leq 15$, the approximate relation is

$$Nu \propto (Pr)^{1/3} \quad (12)$$

Similarly, with $Eu = 1$ for $0.6 \leq Pr \leq 2$ (reference 15, p. 632),

$$Nu \propto (Pr)^{0.4} \quad (13)$$

A similar relation for $Eu = 2$ presumably could be found, but as yet has not been determined.

Effect of Euler number Eu. - The equations that give the effect of the Euler number on the Nusselt number for the case when $T_r \approx 1$, $M \approx 0$, and $\beta = 0$, are given in references 5 and 6. Calculations are made in reference 5 for a series of Prandtl numbers from 0.6 to 1.1 for $Eu = 0$ and $Eu = 1$ and for a series of values of Eu for $Pr = 0.7$ in reference 6. By utilizing the laminar velocity distributions published in reference 17, Nu/\sqrt{Re} may be calculated from the equation given in reference 6, which is

$$\frac{Nu}{\sqrt{Re}} = \frac{\sqrt{\frac{Eu+1}{2}}}{\int_0^\infty \exp(-Pr \int_0^{\bar{\eta}} \bar{f} d\bar{\eta}) d\bar{\eta}} \quad (14)$$

The results of the calculations are shown in figure 3, where $-0.09 \leq Eu \leq 1.5$ and $0.6 \leq Pr \leq 1.1$. The lower value of Eu , where $\partial u/\partial y$ is zero at the wall, gives the largest adverse pressure gradient theoretically possible in a laminar boundary layer with $T_r \approx 1$. If this gradient is exceeded, reverse flow will begin at the wall and transition or separation will occur. When the value of Nu/\sqrt{Re} plotted in figure 3 is defined as F_{lam} , then

$$F_{lam} = Nu/\sqrt{Re} \quad (15)$$

where F_{lam} is a function of both Eu and Pr .

Effect of temperature ratio T_r . - In the following paragraphs, the effect of T_r will be evaluated by keeping ω , φ , and β of equation (8) constant, followed by the evaluation of Nusselt number changes due to variations in ω , φ , and β .

By utilizing figure 4, which is obtained from the results of reference 9, it is seen that at least for $Eu = 0$ the Nusselt number and the temperature ratio may be expressed in the form

$$Nu \propto (T_r)^n \quad (16)$$

Then n can be evaluated from published results for the case when $\beta = 0$ (constant specific heat) and $Eu = 0$ (no pressure gradient). The results of the evaluations where ω and φ were assumed equal are shown in the following table:

T_r range	Mach number	Prandtl number	$\omega = \varphi$	n	Reference
$1 \leq T_r \leq 4$	0	1	0.76	-0.089	2
$1 \leq T_r \leq 4$	0	0.725	.75	-.073	4
$1 \leq T_r \leq 4$.9	.7	.7	-.091	3
$1 \leq T_r \leq 4$	5	1	.8	-.087	3
$1 \leq T_r \leq 2$	5	1	.8	-.084	3

The values in the table indicate that neither changes in the Mach number nor in the Prandtl number have much effect on n in the ranges shown. It will be shown later that this independence is not true of ω . The influence of ω is not shown in the table because the values used in the references cover only a very small range. In practice, ω cannot change much unless extreme temperature ranges are used or unless the fluid is changed.

The wall temperature has been used throughout this investigation in evaluating Nu , Re , and Pr , all of which involve some of the fluid properties. If the free-stream temperature is used instead of the wall temperature for evaluating the fluid properties, the value of n will be quite different. This effect is shown in figure 4. The question immediately arises as to whether there exists some intermediate temperature that, if used for fluid-property evaluation, would cause n to become zero.

It is suggested in reference 9 that some results of Crocco can be closely approximated by evaluating the fluid properties at a temperature T_p when

$$T_p = T_\infty \left[1 + 0.032 M^2 + 0.58 \left(\frac{T_w}{T_\infty} - 1 \right) \right] \quad (17)$$

$$0 < M < 5$$

Because in this correlation constant specific heat ($\beta = 0$), zero pressure gradient ($Eu = 0$), $\omega = 0.75 = \phi$, and $Pr = 0.725$ are assumed, it is not recommended for other cases when these conditions are not fulfilled.

The temperature ratio has another effect not directly related to equation (9), the effect on the stability of the laminar boundary layer. A theoretical analysis is presented in reference 18 and the results are shown in figure 5, where the critical Reynolds number is plotted against the temperature ratio for Euler number of zero. The critical Reynolds number, which indicates the stability of the laminar boundary layer or its resistance to transition, is seen to increase for increasing T_r . It is experimentally shown in reference 19 that the Reynolds number of transition decreases when T_r becomes less than 1.

Effect of viscosity-temperature exponent ω . - In going from one gas to another, the value of ω may change considerably. It is shown in reference 20 that ω ranges from 0.647 for helium at low tempera-

tures to 0.98 for carbon dioxide. Thus a range of values of ω could conceivably be useful. Reference 4 contains such values with $M = 1$, $Pr = 0.725$, $\omega = \phi$, $\beta = 0$, and $Tu = 0$ (presented herein as fig. 6), wherein $c_f \sqrt{Re_{L,\delta}}$, a quantity proportional to Nusselt number divided by $\sqrt{Re_{L,\delta}}$ is plotted against ω . This figure shows that when $T_r = 1$, $Nu_{L,\delta} / \sqrt{Re_{L,\delta}}$ is almost independent of ω . If $T_r = 4$, a change of ω from 0.7 to 0.8 (plausible range when the fluid is air) decreases $Nu_{L,\delta} / \sqrt{Re_{L,\delta}}$ about 3 percent, whereas a change in ω from 0.65 to 1.0 decreases $Nu_{L,\delta} / \sqrt{Re_{L,\delta}}$ about 8 percent, the reference value of $c_f \sqrt{Re_{L,\delta}}$ being at $T_r = 1$.

Effect of thermal conductivity - temperature exponent ϕ . - The separate effect of ϕ has not been published insofar as is known. In the references it is assumed to be the same as ω .

Effect of specific heat - temperature exponent β . - The effect of the exponent β has been computed using the results of reference 4 and is shown in figure 7 with K , a quantity proportional to $Nu_{L,\delta} / \sqrt{Re_{L,\delta}}$, plotted against β . This figure shows that for $T_r = 1$, $Nu_{L,\delta} / \sqrt{Re_{L,\delta}}$ is independent of β . The figure also illustrates the fact that $Nu_{L,\delta} / \sqrt{Re_{L,\delta}}$ decreases for increasing T_r . At $\beta = 0.2$, a plausible value for air, K is reduced 10 percent for $T_r = 4.0$, and inasmuch as $Nu_{L,\delta} / \sqrt{Re_{L,\delta}} \propto K$, $Nu_{L,\delta} / \sqrt{Re_{L,\delta}}$ is also reduced 10 percent from the value at $T_r = 1.0$.

It is therefore apparent that the large changes in the physical properties of the fluid through the boundary layer due to large temperature variations produced several effects. Some of these effects tended to reduce Nu / \sqrt{Re} , whereas other effects tended to increase Nu / \sqrt{Re} . The net result of all these changes has not been completely calculated, but in view of the compensations noted, the net effect may be much less than the changes in the individual properties would indicate.

Effect of Mach number. - Calculations are presented in references 3 and 4 in which a range of Mach numbers was used. From an analysis of the curves based on these calculations, it is concluded that for Mach numbers not exceeding 4 an approximate relation is

$$Nu \propto (1 - CM^2) \quad (18)$$

The coefficient C in equation (18) depends on the other parameters of equation (9), but does not undergo large changes in the range of values usually encountered. The calculated variation caused by changing Mach number from 0 to 2 is shown in figure 4. When $\omega = 0.75 = \varphi$, $Pr = 0.725$, $T_r = 2$, and $\beta = 0 = Eu$, a calculation utilizing the results of reference 4 yields the value 0.00374 for C . This value was altered very little by changing T_r from 1 to 4. The curves of reference 3 indicate a value of 0.00341 for C , where $T_r = 1$, $Pr = 1$, $\omega = 0.8 = \varphi$, and $Eu = 0 = \beta$. Both of these numbers are so small that for subsonic flow, the Mach number effect is quite inappreciable, at least for $Eu = 0$. When $M = 4$, the effect on Nu is to reduce it about 6 percent from the value at $M = 0$.

Correlation equation for laminar flow. - For $1 \leq T_r \leq 4$ and $0 \leq M \leq 2$, the combined effect on the Nusselt number for air as the gas of T_r , M , ω , and β is of the order of a 5- or 10-percent change from the value at $T_r = 1$, $M = 0$ (for air, $\beta = 0.2$ and $\omega = 0.7$). In view of the compensations on Nu/\sqrt{Re} of the different factors involved, an approximation has been made for purposes of correlation for the heat transfer from a laminar boundary layer. For this approximation, equation (9) takes the form

$$Nu = \psi_3 (Re, Pr, Eu) \quad (18a)$$

Figure 3 was put in the form of figure 8 by using the results of figure 3 for Prandtl number of 0.7 and results of reference 6 for $Eu > 1.5$. For the range $0 \leq Eu \leq 2$, the results shown in figure 8 check figure 3 to less than 3 percent. Thus the following equation replaces equation (15) for $0.6 \leq Pr \leq 1$ and $0 \leq Eu \leq 2$:

$$Nu/(Pr)^{1/3} = \bar{F}_{lam} \sqrt{Re} \quad (19)$$

where

$$\bar{F}_{lam} = F_{lam}/(Pr)^{1/3}$$

Equation (19) will be the correlation equation for laminar flow with \bar{F}_{lam} given in figure 8.

Equations of Turbulent Boundary Layer

When the boundary layer becomes turbulent, the differential equations (2) to (4) can no longer be applied because the motion is not steady and the mean motion does not satisfy the equation of Stokes. In spite of much simplification, neither the dynamic nor the thermal problems are at present amenable to solution in their more exact form. The flow is often regarded as consisting of a mean flow and a superposed fluctuating motion. By use of this concept, equations similar to equations (2) and (4) have been presented wherein the velocities and the temperatures are time averages (reference 8) that neglect pressure-gradient and dissipation terms as follows:

$$\bar{u} \frac{\partial \bar{u}}{\partial x} + \bar{v} \frac{\partial \bar{u}}{\partial y} = + \frac{\partial}{\partial y} \left(\frac{\mu}{\rho} \frac{\partial \bar{u}}{\partial y} + \epsilon_M \frac{\partial \bar{u}}{\partial y} \right) \quad (20)$$

$$J \left(\bar{u} \frac{\partial \bar{T}}{\partial x} + \bar{v} \frac{\partial \bar{T}}{\partial y} \right) = \frac{\partial}{\partial y} \left(\frac{\mu}{\rho \text{Pr}} \frac{\partial \bar{T}}{\partial y} + \epsilon_H \frac{\partial \bar{T}}{\partial y} \right) \quad (21)$$

where ϵ_M is the so-called eddy diffusivity for momentum and ϵ_H is the so-called eddy diffusivity for heat. Thus formally, the laminar solutions for no pressure gradient and no dissipation could be used by substituting $\epsilon_M + \mu/\rho$ for μ/ρ and $\epsilon_H + \mu/\rho \text{Pr}$ for $\mu/\rho \text{Pr}$. This solution cannot be carried out so simply, however, because the values of the eddy diffusivities vary from place to place. Consequently, equations (20) and (21) have been used to derive Reynolds analogy. This derivation is carried out by postulating that $\partial p/\partial x = 0$, $\text{Pr} = 1$, and $\epsilon_M = \epsilon_H$. Equations (20) and (21) then become identical in form, the only difference being the substitution of T in equation (21) for u in equation (20) as the dependent variable. It can then be shown (reference 8) that

$$\frac{H}{c_{p,w} \rho_w U} = \frac{f}{2} \quad (22)$$

where f is the friction coefficient equal to $\frac{\tau_w}{\rho_s U^2/2}$

The postulate that $\text{Pr} = 1$ holds approximately for all gases. A number of formulas have been proposed for correcting equation (22) for cases where $\text{Pr} \neq 1$. The simplest formula, given in reference 21, is

$$\frac{h}{c_{p,w} \rho_w U} (\text{Pr})^{2/3} = \frac{f}{2} \quad (23)$$

It is shown in reference 8 that equations containing more accurate and more complex correction factors do not differ markedly from equation (23) in the range $0.5 < \text{Pr} < 10$. When equation (23) is solved for Nu , the result is

$$\text{Nu} = \frac{f}{2} \text{Re} (\text{Pr})^{1/3} \quad (24)$$

The correlation for Nu can then be completed by substituting an f correlation in equation (24). One of the simplest of these correlations is given in reference 8 and is

$$\frac{f}{2} = 0.0296 (\text{Re})^{-0.2} \quad (25)$$

Substitution of this value in equation (24) yields

$$\text{Nu} = 0.0296 (\text{Re})^{0.8} (\text{Pr})^{1/3} \quad (26)$$

Reference 9 presents equation (26), compares it with two more elaborate correlations, and concludes that equation (26) is adequate for gases, though possibly not for liquids with extreme values of Pr . Accordingly, equation (26) will be used as the correlation equation for turbulent boundary layers even though the pressure-gradient effect has not been included.

In the laminar boundary layer, it was found that the wall temperature was suitable for evaluating the gas properties ρ , c_p , μ , and k . Although the evaluation temperature for a turbulent boundary layer cannot be obtained from this analysis, a temperature equal to the surface temperature is suggested, considering that the laminar sublayer in the turbulent boundary layer may be controlling the heat transfer. Also, good correlation for turbulent flow in pipes is obtained in reference 22 when the gas properties are evaluated at the wall temperature. The wall temperature will therefore be used for evaluating the gas properties in both laminar and turbulent boundary layers.

Heat Transfer with Both Laminar and Turbulent Boundary Layers

As the solid surface increases in length, the Reynolds number becomes larger and the laminar layer ultimately becomes unstable, changing to a turbulent boundary layer. The problem then arises of computing an average Nusselt number for the whole body, from the stagnation point where $x = 0$ to the trailing edge where $x = L$. If the transition point is at ξL , where the laminar boundary layer changes to a turbulent boundary layer, then

$$\xi = \frac{L_{tr}}{L} \quad (27)$$

The method for obtaining the total heat transfer is to integrate H for both laminar and turbulent boundary layers.

$$\int_0^{L_{tr}} H dx + \int_{L_{tr}}^L H dx = \bar{H} L \quad (28)$$

The heat transfer over the whole surface will be obtained when both laminar and turbulent boundary layers are considered to exist on the surface.

Heat transfer through laminar boundary layer. - The correlation equation for the laminar boundary layer is given as equation (19), which may be written as

$$\frac{H}{k_w (Pr)^{1/3}} = \bar{F}_{lam} \sqrt{\frac{\rho_w U}{\mu_w}} x^{-1/2} \quad (29)$$

In order to obtain the heat transferred, an integration over the laminar layer is necessary. The assumption of constant ρ_w will be made, which is reasonable for low Mach numbers. In addition, the wall temperature and \bar{F}_{lam} will be assumed constant over the laminar portion. Then integration of equation (29) yields

$$\frac{1}{k_w(\text{Pr})^{1/3}} \int_0^{L_{\text{tr}} = \xi L} H dx = \bar{F}_{\text{lam}} \sqrt{\frac{\rho_w}{\mu_w}} \int_0^{L_{\text{tr}} = \xi L} \sqrt{\frac{U}{x}} dx \quad (30)$$

It is stated in references 5 and 6 that if Eu is to be constant, the relation between U and x is

$$U = c_1 x^{Eu} \quad (31)$$

where Eu is the Euler number. Substituting equation (31) in equation (30) and integrating yield

$$\frac{1}{k_w(\text{Pr})^{1/3}} \int_0^{\xi L} H dx = \frac{2 \bar{F}_{\text{lam}}}{Eu+1} \sqrt{\frac{\rho_w c_1}{\mu_w}} (\xi L)^{\frac{Eu+1}{2}} \quad (32)$$

Heat transfer through turbulent boundary layer. - The correlation equation for the turbulent boundary layer is given as equation (26), which may be written as

$$\frac{H}{k_w(\text{Pr})^{1/3}} = 0.0296 \left(\frac{U_p}{\mu_w} \right)^{0.8} x^{-0.2} \quad (33)$$

Proceeding in a manner similar to equations (29) to (32), with the integration now from ξL to L , equation (33) becomes (neglecting pressure-gradient effects on the local heat-transfer coefficient)

$$\frac{1}{k_w(\text{Pr})^{1/3}} \int_{\xi L}^L H dx = \frac{0.0296}{0.8(Eu+1)} \left(\frac{c_1 \rho_w}{\mu_w} \right)^{0.8} L^{0.8(Eu+1)} \left[1 - \xi^{0.8(Eu+1)} \right] \quad (34)$$

Summation of heat transfer over surface length L . - Where both laminar and turbulent boundary layers exist over the surface, use of equations (28), (32), and (34) will yield an average heat-transfer coefficient, thus

$$\frac{\bar{h}L}{k_w(\text{Pr})^{1/3}} = \frac{2\bar{F}_{\text{lam}}}{Eu+1} \sqrt{\frac{\rho_w c_1}{\mu_w}} \left(\frac{\xi L}{2}\right)^{\frac{Eu+1}{2}} + \frac{0.037}{Eu+1} \left(\frac{c_1 \rho_w}{\mu_w}\right)^{0.8} L^{0.8(Eu+1)} \left[1 - \xi^{0.8(Eu+1)}\right] \quad (35)$$

The left side of equation (35) is $\bar{Nu}_L/(\text{Pr})^{1/3}$, the ordinate customarily used in experimental correlations. The right side is usually given as a function of a Reynolds number. A suitable Reynolds number for use with $\bar{U}L$ is

$$\frac{\bar{U} \rho_w L}{\mu_w} = \bar{Re}_L \quad (36)$$

where \bar{U} is the average velocity over the solid surface. It is necessary to express c_1 in terms of \bar{U} .

The defining equation for \bar{U} is

$$\bar{U}L = \int_0^L U \, dx \quad (37)$$

Substitution in equation (37) of $U = c_1 x^{Eu}$ and integration yields

$$c_1 = \frac{(Eu+1) \bar{U}}{L^{Eu}} \quad (38)$$

Substitution of this value of c_1 in equation (35) yields

$$\frac{\bar{Nu}_L}{(\text{Pr})^{1/3}} = \frac{2\bar{F}_{\text{lam}}}{\sqrt{Eu+1}} \sqrt{\bar{Re}_L} \xi^{\frac{Eu+1}{2}} + \frac{0.037}{(Eu+1)^{0.2}} \bar{Re}_L^{0.8} \left[1 - \xi^{0.8(Eu+1)}\right] \quad (39)$$

The reference length used in the Nusselt and Reynolds numbers is sometimes different from the L used here. For turbine-blade shapes, a common reference length is perimeter/ π , which reduces to the

diameter for a circular cylinder. In equation (39), perimeter/ π will be used by substituting $2L/\pi$ for L in Nu_L and in Re_L . The coefficient 2 in the first term then becomes $2\sqrt{2/\pi}$ or 1.596, whereas the coefficient 0.037 in the second term becomes $0.037 (2/\pi)^{0.2}$ or 0.0338.

If values are chosen for Eu and ξ , then $Nu_p / (Pr)^{1/3}$ is a function of Re_p . Even when plotted on a logarithmic scale, the function will still be slightly curved because of the 0.5 and 0.8 powers of the Reynolds number in equation (39). Because heat-transfer correlations are usually presented by drawing a straight line through the observed points plotted on a logarithmic scale, for purposes of comparison equation (39) will be put into the approximate form

$$Nu_p / (Pr)^{1/3} = \bar{F} (Re_p)^Z \quad (40)$$

with perimeter/ π being the reference length.

Equation (39) can be put into the form of equation (40) by making the exact equation (39) coincide with the approximate equation (40) at two points near the ends of the observed range of experimental data. In this case, the two points chosen will be $Re_p = 2 \times 10^4$ and 2×10^5 . The greatest difference between the exact and approximate curves will then be about 2 percent or less for $10^4 \leq Re_p \leq 4 \times 10^5$, increasing to about 6 percent when Re_p is extended to 10^6 .

Values of Z and \bar{F} are shown in figure 9. They are plotted as ordinates against the transition ratio ξ as abscissa. Four values of Eu are shown, ranging from -0.09 to 2. The effect of Eu in figure 9 is less than that shown in figure 8 because Eu appears in the denominator of the first term of equation (39) and thus partly cancels the effect of \bar{F}_{lam} .

By using figure 9 and equation (40), curves were determined for different values of ξ and Eu , as shown in figure 10, where $Nu_p / (Pr)^{1/3}$ is plotted against Re_p . As would be expected, the lowest heat transfer results from a completely laminar boundary layer, $\xi = 1$; whereas the highest heat transfer is obtained for an

entire turbulent boundary layer, $\xi = 0$. In practice, some of the curves would not extend into all the Reynolds number ranges shown, but the extension has been made in figure 10 to illustrate the theoretical trends. It is seen from the slope of these theoretical curves why experimental results, when plotted in this fashion, often-times yield slopes different from 0.5 or 0.8, the theoretical values expected with either completely laminar or turbulent boundary layers, respectively.

APPLICATION OF THEORY TO EXPERIMENTAL RESULTS

In the following section, the theory will be compared with experimental results obtained from cylinders, an airfoil, and turbine-blade cascades. On these surfaces, Eu varies locally but average values will be used except for stagnation points and the airfoil where local heat-transfer coefficients have been measured and can be compared with theory.

Cylinders

Equation (19), when written in the form

$$\frac{Hx}{k_w} = \bar{F}_{lam} (Pr)^{1/3} \sqrt{\frac{\rho U_x}{\mu_w}} \quad (41)$$

can be used to calculate a Nusselt number for the stagnation point of a cylinder. Near this point, it has been shown (reference 23) that

$$U = 3.63 \frac{U_1 x}{D} \quad (42)$$

where D is the cylinder diameter and U_1 the upstream velocity of the fluid. Substitution of equation (42) in equation (41), cancellation of the x 's, and multiplication of both sides by D yield

$$\frac{HD}{k_w} = 1.905 \bar{F}_{lam} (Pr)^{1/3} \sqrt{\frac{\rho U_1 D}{\mu_w}} \quad (43)$$

For this case, $Eu = 1$ (reference 15, p. 631) and utilizing figure (8) for \bar{F}_{lam} with $Pr = 0.7$, equation (43) becomes

$$Nu_D = 0.945 \sqrt{Re_D} \quad (44)$$

or

$$Nu_D / (Pr)^{1/3} = 1.064 \sqrt{Re_D} \quad (45)$$

Equation (44) is nearly the same as that given in reference 15 (p. 632). The difference in the numerical coefficient (1.01) in the reference is due to the use of a higher Prandtl number ($Pr = 0.733$) and a theoretical velocity distribution ($U = 4U_1 x/D$).

Experimental measurements of the Nusselt number at the stagnation point of a cylinder are given in reference 24 and are plotted in figure 11 for three cylinders of diameters 1.27, 2.54, and 6.35 inches. The theoretical curve is shown also and agrees very well with the data.

The average Nusselt numbers over the cylinders are shown in figure 12, together with the theoretical curve from equation (40). The Reynolds number Re_D containing the upstream velocity U_1 has been converted to the Reynolds number Re_p , which contains \bar{U} , the average velocity around the cylinder. The average velocity and the dimensionless number Eu were found from the pressure distributions given in reference 24 through use of Bernoulli's equation and the definition of the Euler number. The value of ξ was obtained by noting the point of minimum Nusselt number in the plot of Nu against the angle measured from the stagnation point. Thus, ξ was found to be $82^\circ/180^\circ$ or 0.455. The agreement between the experiment and the theory is surprisingly good in view of the fact that separation has occurred on the cylinder and no account of separation was taken in the theoretical development.

Airfoil

Reference 25 gives local heat-transfer coefficients for clear-air conditions obtained in flight investigations of a NACA 65,2-016 symmetrical airfoil with an 8-foot chord. An equivalent diameter at the leading edge was obtained herein using the coordinate system for the airfoil given in reference 26. From this equivalent diameter and the data of reference 25, it was possible to determine $Nu_D / (Pr)^{1/3}$ and Re_D at the stagnation point. Because

only one flight speed was used for the clear-air condition, only one point was obtained, which is shown in figure 11 and agrees well with the theoretical curve and experimental results from cylinders.

Using the experimental results of reference 25, it was also possible to determine local Nusselt, Reynolds, Prandtl, and Euler numbers. The coefficient F_{lam} could then be determined locally from the Euler number and a theoretical curve drawn for comparison with the experimental results. The comparison is made in figure 13, equation (19) being for the laminar case and equation (26) for the turbulent case. The curve for a flat plate is given for the laminar range to show the increase resulting from inclusion of Euler number effects in equation (19). A scale is also given for the variation of x/L with Re . It is seen that equation (19) agrees well with the data in the laminar range until very close to the leading edge. Equation (26) falls somewhat below the experimental results.

An average value of $Nu_p / (Pr)^{1/3}$ was calculated using equation (40) and figure 9. The average Euler number was obtained from the pressure distribution and the transition ratio was obtained from the plot of local heat-transfer coefficient against x/L . The transition point was taken as the value of x/L where the heat-transfer coefficient shows a sharp increase. By using this method, the calculated value of $Nu_p / (Pr)^{1/3}$ was about 9 percent less than the experimental value.

Turbine-Blade Cascades

In order to determine average outside coefficients for turbine blades, various sets of heat-transfer measurements have been assembled. The pertinent facts about these experiments are shown in table I. It is evident from the table that various pressures, temperatures, velocities, and lengths were used by the different authors in their correlations. In order to put these results on a uniform and comparable basis, the gas properties were all reduced to those at blade temperatures, the velocities were reduced to average values around the blade periphery outside the boundary layer, and the reference length was reduced to $perimeter/\pi$. The velocity reduction was accomplished by using the state of the gas at the inlet to the blade cascade, calculating the velocity distribution around the blades through use of the stream-filament method, and then utilizing the experimental curves and the data where available to obtain

$Nu_p / (Pr)^{1/3}$. The details of these calculations are given in refer-

ence 14. Some of the experimental correlations resulting are shown in figure 14.

1346 The comparisons between the correlation curves given in figure 14 and the theory are made in figures 15 to 17. The method used to obtain the theoretical curves is given in appendix B. The comparisons indicate better agreement of the theory and the experiment when ξ is determined by the condition that $Eu = 0$ rather than by the condition that $Eu = -0.09$. An exception is the case of reference 13 (fig. 17), where better agreement is obtained for the $Eu = -0.09$ condition. The deviation between the ξ determinations in this example, however, is rather small.

SUMMARY OF RESULTS

From a theoretical analysis of heat transfer from the boundary-layer aspect, the following results were obtained:

1. Other dimensionless numbers in addition to the Reynolds and Prandtl numbers are needed for an accurate evaluation of the Nusselt number. Two of the most influential numbers are: the Euler number, a measure of the pressure gradient; and the transition ratio, which measures the amount of laminar boundary layer present on a surface.
2. The Mach number appeared to have a smaller effect, at least for Mach numbers less than 2 and temperature ratios between 1 and 4, when the fluid was air. The viscosity- and specific heat-temperature exponents showed varying influence, depending on the temperature ratio.
3. An equation for the average heat transfer was derived for constant wall temperature to include the Euler number and transition-ratio effects.
4. Theoretical curves based on this analysis agreed with experimental results obtained from cylinders, a symmetrical airfoil, and turbine-blade cascades.

Lewis Flight Propulsion Laboratory,
National Advisory Committee for Aeronautics,
Cleveland, Ohio.

APPENDIX A

SYMBOLS

The following symbols are used in this report:

- a speed of sound in gas
- C factor in correlation equation (18), $Nu \propto (1 - C M^2)$
- c_f drag coefficient due to skin friction
- c_p specific heat at constant pressure at point x, y in boundary layer
- c_1 factor in $U = c_1 x^{Eu}$
- D diameter of cylinder
- D_o characteristic length, $\frac{2L}{\pi}$
- Eu Euler number, $-\frac{\partial p / \partial x}{\rho_o U^2 / x}$
- \bar{F} mean coefficient, $\frac{\bar{Nu}_p}{Re_p Z (Pr)^{1/3}}$
- F_{lam} coefficient for laminar flow, $\frac{Nu}{\sqrt{Re}}$
- \bar{F}_{lam} mean coefficient, $\frac{F_{lam}}{(Pr)^{1/3}}$
- f friction coefficient, $\frac{\tau_w}{\rho_o U^2 / 2}$
- \bar{f} nondimensional stream function, $\sqrt{\frac{Eu+1}{2}} \frac{q}{\sqrt{Ux v}}$

- 1346
- g acceleration due to gravity
- H outside heat-transfer coefficient
- \bar{H} mean outside heat-transfer coefficient
- h enthalpy
- J mechanical equivalent of heat
- K from reference 4, $K = \frac{h_w - h_\delta}{(T_w - T_\delta) c_{p,\delta}}$
- k thermal conductivity at point x, y in boundary layer
- L total length of surface, measured along surface from stagnation point to trailing edge
- L_{tr} value of x at transition point
- M Mach number, U/a
- Nu local Nusselt number based on x, Hx/k_w
- Nu_D local Nusselt number based on D, HD/k_w
- \bar{Nu}_L mean Nusselt number based on L, \bar{HL}/k_w
- \bar{Nu}_p mean Nusselt number based on $\frac{\text{perimeter}}{\pi}$, \bar{HD}_o/k_w
- n exponent of Nusselt - temperature-ratio relation, $Nu \propto (T_r)^n$
- Pr Prandtl number, $c_{p,w} \mu_w / k_w$
- p static pressure in boundary layer, or at its edge because $\partial p / \partial y$ is assumed zero
- q stream function of flow in boundary layer
- R universal gas constant
- Re local Reynolds number based on x, $U_{p,w} x / \mu_w$

Re_{cr}	critical Reynolds number below which all oscillations in laminar boundary layer are damped
Re_D	Reynolds number based on D , $U_1 \rho_w D / \mu_w$
\overline{Re}_L	mean Reynolds number based on L , $\overline{U}_w L / \mu_w$
\overline{Re}_p	mean Reynolds number based on $\frac{\text{perimeter}}{\pi} \frac{\overline{U}_w D_o}{\mu_w}$
T	gas temperature at point x, y in boundary layer
\overline{T}	time average temperature
T_p	reference temperature for property values, $T_\delta \left[1 + 0.032 M^2 + 0.58 \left(\frac{1}{T_r} - 1 \right) \right]$
T_r	temperature ratio, T_δ / T_w
U	velocity of gas at edge of boundary layer
\overline{U}	integrated average velocity U
U_1	velocity upstream of body
u	boundary-layer velocity in x direction
\overline{u}	time-average boundary-layer velocity in x direction
v	boundary-layer velocity in y direction
\overline{v}	time-average boundary-layer velocity in y direction
x	distance along surface or parallel to it
y	distance normal to surface
Z	exponent of Reynolds number (equation (40))

- 1346
- β exponent in specific heat - temperature relation,

$$c_p / c_{p,w} = (T/T_w)^\beta$$
- δ outer edge of boundary layer
- ϵ_H eddy diffusivity for heat
- ϵ_M eddy diffusivity for momentum
- $\bar{\eta}$ nondimensional boundary-layer coordinate, $\sqrt{\frac{Eu+1}{2}} y \sqrt{\frac{U}{\nu x}}$
- Λ recovery factor, $\frac{T_e - T_\delta}{U^2 / 2gc_p}$
- μ absolute viscosity of gas at point x, y in boundary layer
- ν kinematic viscosity (μ/ρ)
- ξ transition ratio, $\frac{L_{tr}}{L}$
- ρ density of gas at point x, y in boundary layer
- τ_w shear stress, $(\mu \partial u / \partial y)_w$
- φ exponent in thermal conductivity-temperature relation,

$$k/k_w = (T/T_w)^\varphi$$
- ψ function, equation (5)
- ψ_1 function, equation (9)
- ψ_2 function, equation (10)
- ψ_3 function, equation (18a)
- ω exponent in viscosity-temperature relation, $\mu/\mu_w = (T/T_w)^\omega$

Subscripts:

D based on diameter
e effective
L based on total length
lam laminar
P pressure surface
p based on perimeter
S suction surface
SP suction and pressure surface
w wall condition
δ main stream condition

APPENDIX B

METHOD OF EVALUATING TRANSITION RATIO AND AVERAGE EULER NUMBER

In order to obtain the theoretical curves for comparison with experimental correlations shown in figure 14, the chordwise velocity distributions given in reference 14 were used to determine the point of transition and the average value of the Euler number, inasmuch as

$$Eu = - \frac{dp/dx}{\rho_{\delta} U^2/x} \quad (B1)$$

and from Bernoulli's equation

$$- \frac{dp}{dx} = \rho_{\delta} U \frac{dU}{dx}$$

Equation (B1) becomes

$$Eu = \frac{x}{U} \frac{dU}{dx} \quad (B2)$$

By using finite differences, dU/dx was calculated from the aforementioned velocity distribution and combined with the other factors in equation (B2) to obtain Eu . The resultant plot of Eu against x/L is shown in figure 18 using the velocity distribution of reference 12 given in reference 14. As shown in figure 18, the transition point was obtained at x/L , where $Eu = 0$ or $Eu = -0.09$ for both the suction and pressure surfaces. The value $Eu = -0.09$ represents the condition where the adverse pressure gradient is so large that reverse flow at the wall is imminent. The value $Eu = 0$ represents the limit of the adverse pressure region. At any value of Eu less than $Eu = 0$, the boundary-layer velocity profile has a point of inflection, indicating an unstable velocity regime.

A weighted average of the transition ratio was determined using the lengths of the suction and pressure surfaces.

$$\xi = \frac{L_S \xi_S + L_P \xi_P}{L_S + L_P} \quad (B3)$$

The Euler number was determined by obtaining the integrated average value of Eu to the point of transition for both the suction and pressure surfaces. A weighted average was also used for the Euler number.

$$Eu_{SP} = \frac{L_S Eu_S + L_P Eu_P}{L_S + L_P} \quad (B4)$$

Using the values of ξ and Eu_{SP} calculated by equations (B3) and (B4), figure 8 was utilized to determine Z and \bar{F} and these values substituted in equation (40) to give the theoretical curve.

REFERENCES

1. Pohlhausen, E.: Der Wärmeaustausch zwischen festen Körpern und Flüssigkeiten mit kleiner Reibung und kleiner Wärmeleitung. Z.f.a.M.M., Bd. 1, Heft 2, 1921, S. 115-121.
2. von Kármán, Th., and Tsien, H. S.: Boundary Layer in Compressible Fluids. Jour. Aero. Sci., vol. 5, no. 6, April 1938, pp. 227-232.
3. Hantzsche, and Wendt: The Laminar Boundary Layer in Compressible Flow along a Flat Plate with and without Transfer of Heat. Volkenrode Trans. No. MOS 53, British R.A.E.
4. Crocco, Luigi: The Laminar Boundary Layer in Gases. Trans. No. F-TS-5053-RE, ATI No. 28323, CADO, Air Materiel Command (Wright Field).
5. Tifford, Arthur N.: The Thermodynamics of the Laminar Boundary Layer of a Heated Body in a High-Speed Gas Flow Field. Jour. Aero. Sci., vol. 12, no. 2, April 1945, pp. 241-251.
6. Eckert, E., and Drewitz, O.: Calculation of the Temperature Field in the Laminar Boundary of an Unheated Body in a High Speed Flow. R.T.P. Trans. No. 1594, British M.A.P.
7. Chapman, Dean R., and Rubesin, Morris W.: Temperature and Velocity Profiles in the Compressible Laminar Boundary Layer with Arbitrary Distribution of Surface Temperature. Jour. Aero. Sci., vol. 16, no. 9, Sept. 1949, pp. 547-565.

- 1346
8. Boelter, L. M. K., Grossman, L. M., Martinelli, R. C., and Morrin, E. H.: An Investigation of Aircraft Heaters. XXIX - Comparison of Several Methods of Calculating Heat Losses from Airfoils. NACA TN 1453, 1948.
 9. Johnson, H. A., and Rubesin, M. W.: Aerodynamic Heating and Convective Heat Transfer - Summary of Literature Survey. Trans. ASME, vol. 71, no. 5, July 1949, pp. 447-456.
 10. Seban, R. A.: An Analysis of Heat Transfer to Turbulent Boundary Layers in High Velocity Flow. Paper No. 48-A-44, presented before Ann. Meeting A.S.M.E. (New York), Nov. 28-Dec. 3, 1948.
 11. Pollmann, Erich: Temperatures and Stresses on Hollow Blades for Gas Turbines. NACA TM 1183, 1947.
 12. Meyer, Gene L.: Determination of Average Heat-Transfer Coefficients for a Cascade of Symmetrical Impulse Turbine Blades. I - Heat Transfer from Blades to Cold Air. NACA RM E88L2, 1948.
 13. Andrews, S. J., and Bradley, P. C.: Heat Transfer to Turbine Blades. Memo No. M.37, Nat. Gas Turbine Establishment, M.A.P. (London), Oct. 1948.
 14. Hubbarth, James E.: Comparison of Outside-Surface Heat-Transfer Coefficients for Cascades of Turbine Blades. NACA RM E50C28.
 15. Goldstein, Sidney: Modern Development in Fluid Dynamics.. Vols. I and II. Clarendon Press (Oxford), 1938.
 16. Keenan, Joseph H., and Kaye, Joseph: Gas Tables. John Wiley & Sons, Inc., 1948.
 17. Hartree, D. R.: On an Equation Occurring in Falkner and Skan's Approximate Treatment of the Equations of the Boundary Layer. Proc. Cambridge Phil. Soc., vol. 33, pt. 2, April 1937, pp. 223-239.
 18. Lees, Lester: The Stability of the Laminar Boundary Layer in a Compressible Fluid. NACA Rep. 876, 1947. (Formerly NACA TN 1196.)
 19. Liepmann, Hans W., and Fila, Gertrude H.: Investigations of Effects of Surface Temperature and Single Roughness Elements on Boundary-Layer Transition. NACA Rep. 890, 1947.

20. Jeans, J. H.: The Dynamical Theory of Gases. Cambridge Univ. Press, 2d ed., 1916, p. 302.
21. Colburn, Allan P.: A Method of Correlating Forced Convection Heat Transfer Data and a Comparison with Fluid Friction. Trans. Am. Inst. Chem. Eng., vol. XXIX, 1933, pp. 174-210.
22. Lowdermilk, Warren H., and Grele, Milton D.: Heat Transfer from High-Temperature Surfaces to Fluids. II - Correlation of Heat-Transfer and Friction Data for Air Flowing in Inconel Tube with Rounded Entrance. NACA RM E8L03, 1949.
23. Eckert, E.: Calculation of the Heat Transfer in the Boundary Layer of Bodies in Flow. AFI Trans. No. 143691, CADO (Wright-Patterson Air Force Base).
24. Schmidt, Ernst, and Wenner, Karl: Heat Transfer over the Circumference of a Heated Cylinder in Transverse Flow. NACA TM 1050, 1943.
25. Neel, Carr B., Jr., Bergrun, Norman R., Jukoff, David, and Schlaff, Bernard A.: The Calculation of the Heat Required for Wing Thermal Ice Prevention in Specified Icing Conditions. NACA TN 1472, 1947.
26. Abbott, Ira H., von Doenhoff, Albert E., and Stivers, Louis S., Jr.: Summary of Airfoil Data. NACA Rep. 824, 1945.

TABLE I - SUMMARY OF VARIABLES USED IN HEAT-TRANSFER EXPERIMENTS ON OUTSIDE OF TURBINE BLADES

Investigator Reference number	Pollmann 11	Meyer 12	Andrews, Bradley 13
Temperature ratio, T_r	0.8	0.9	2 - 1
Evaluation temperature for: viscosity	Inlet stream	Film ¹	Blade
density	Inlet stream	Inlet stream	Mean ²
thermal conductivity	Inlet stream	Film ¹	Blade
Pressure for density	Inlet	Inlet	Mean ²
Velocity	Inlet	Inlet	Exit
Length	Perimeter/ π	Perimeter/ π	Chord
Chord, in.	3.94	0.680	1.0
Number of blades	3	6	5
Solidity ³	1.47	1.92	1.61
Method of heating or cooling	Electrically heated blade	Electrically heated blades	Hot gas stream with water-cooled blade
Remarks	Only middle blade heated	Blades heated by conduction	Only middle blade cooled

¹ Film temperature = $1/2$ (stream static temperature + wall temperature).

² Mean density = $\bar{p}/R\bar{T}_{mean}$

$\bar{p} = 1/2$ (inlet pressure + exit pressure) from cascade

$T_{mean} = 1/2 (T_e + T_w)$, $T_e = T_\delta + 0.85 U^2/2gJc_p$

³ Solidity = chord/spacing

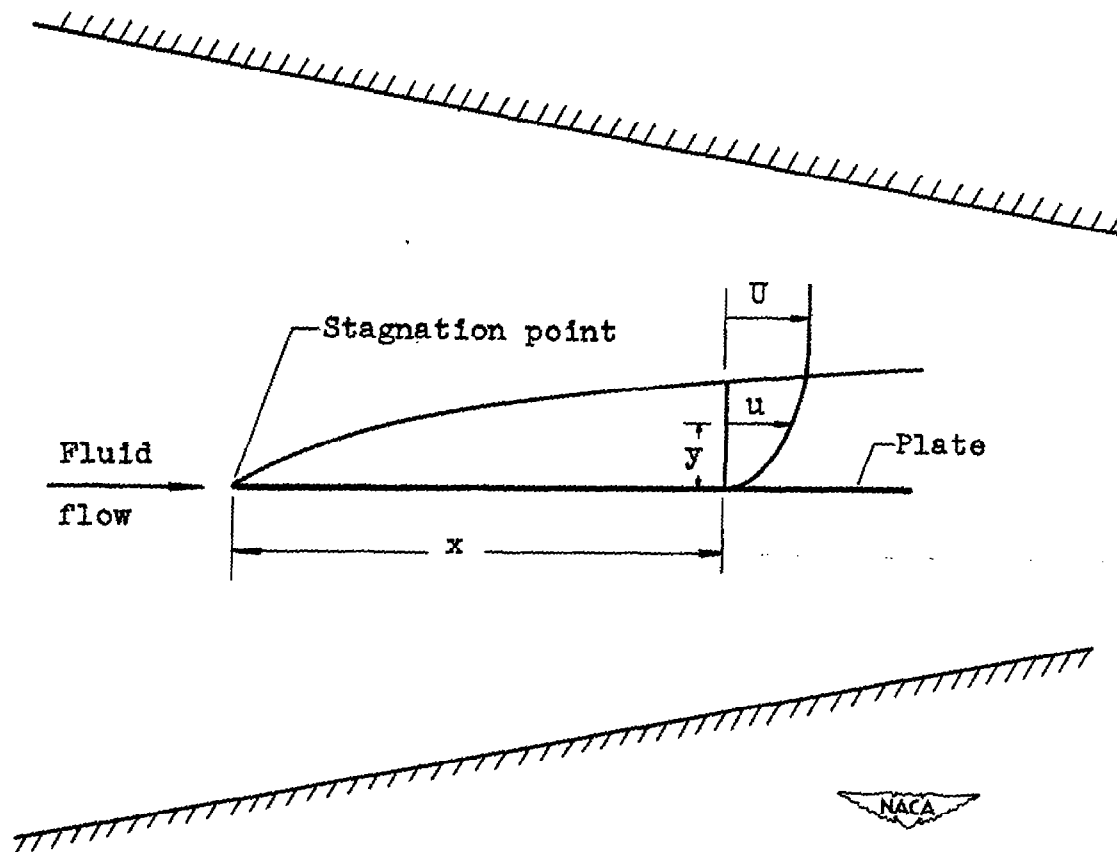


Figure 1. - Diagram of boundary layer.

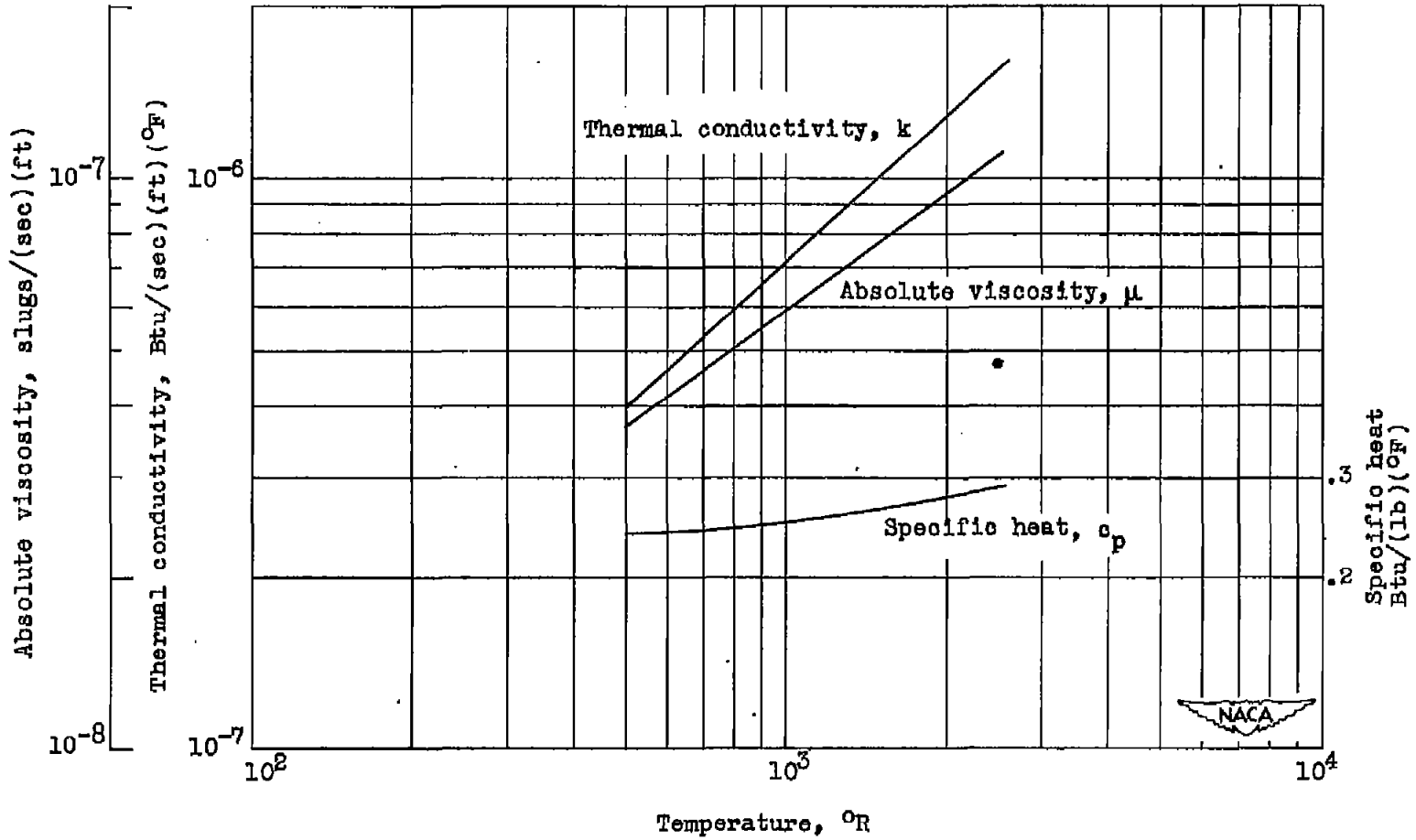


Figure 2. - Temperature effect on the properties of air (reference 16).

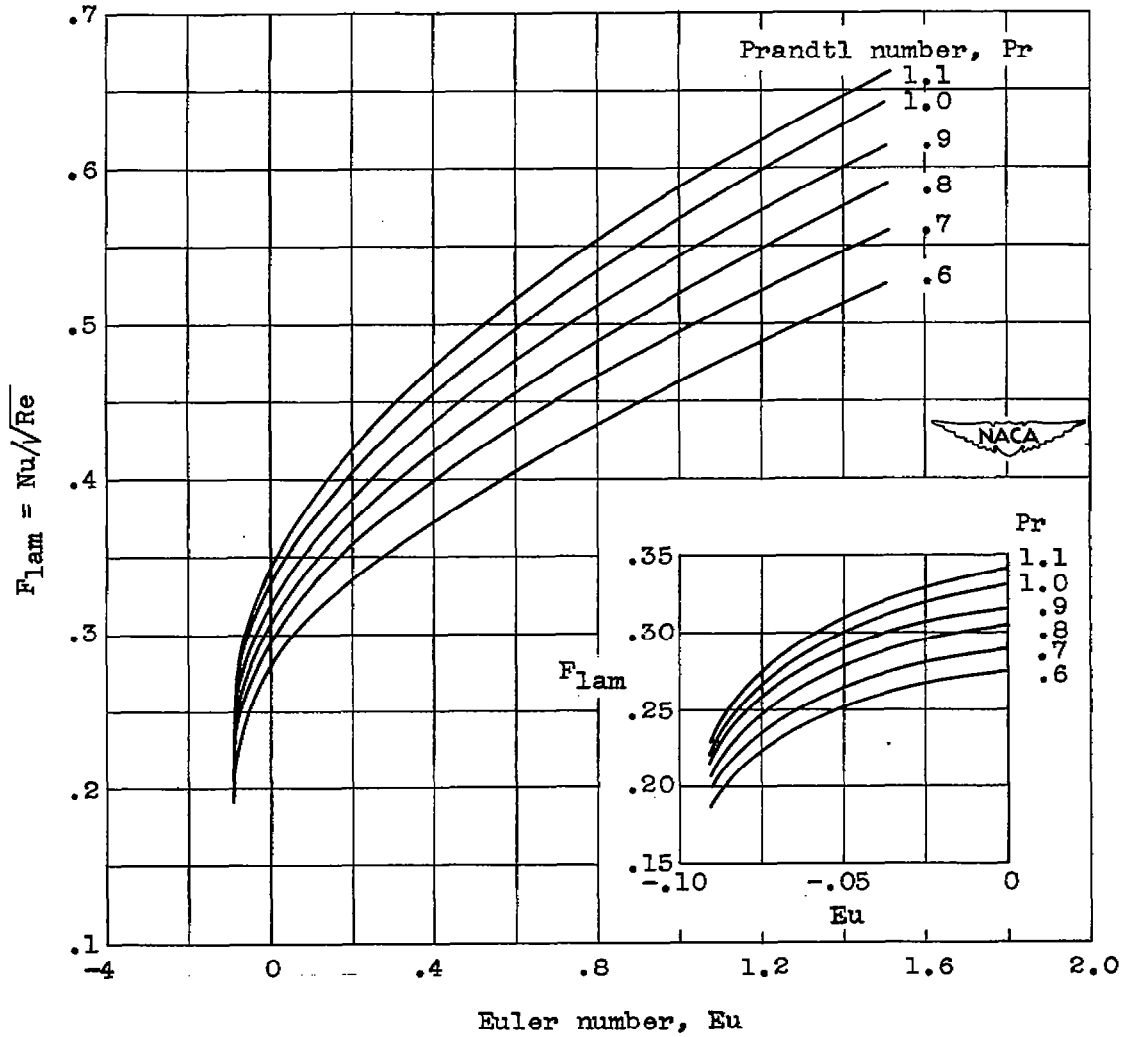
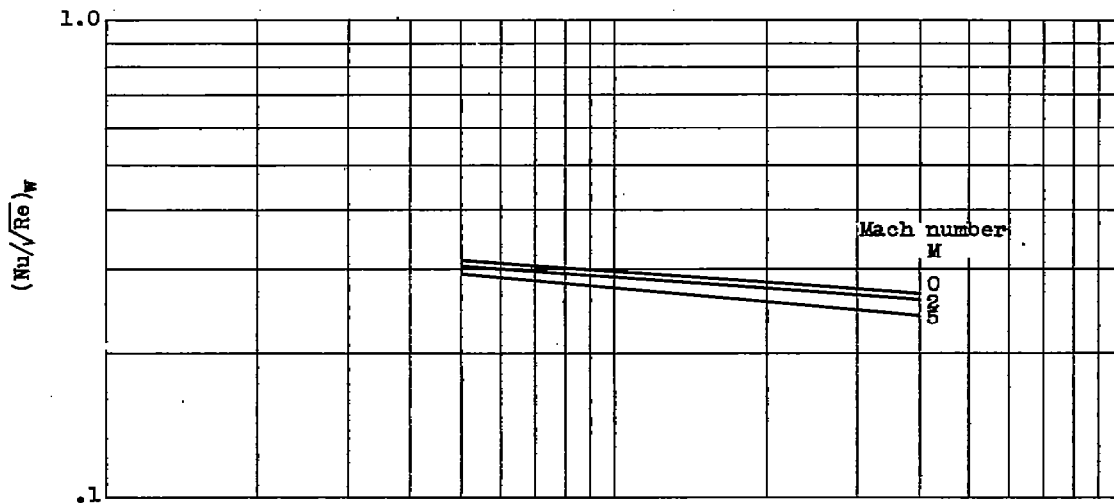
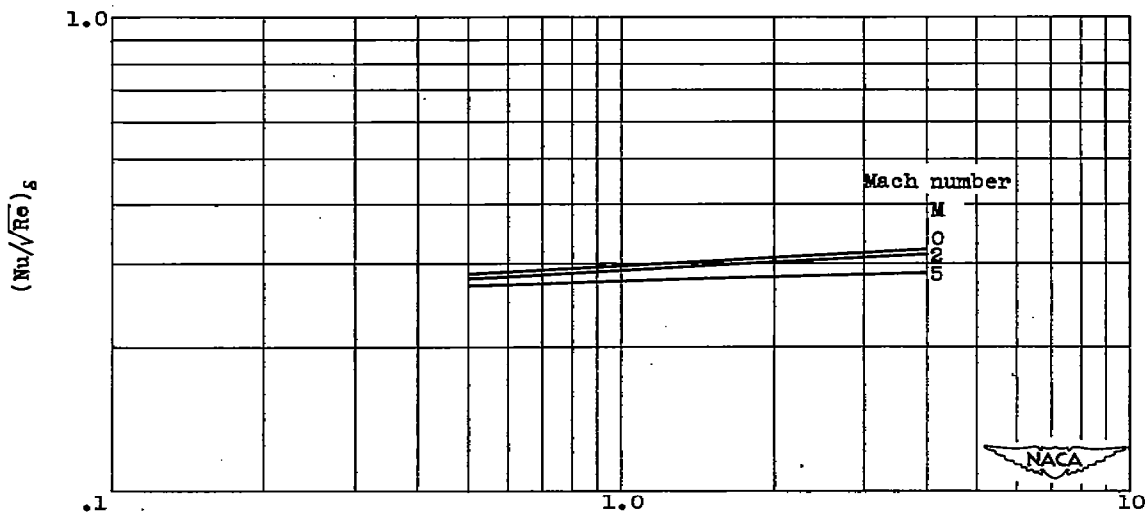


Figure 3. - Theoretical effect of Euler number and Prandtl number on heat transfer with laminar boundary layer. $T_r \approx 1$; $M \approx 0$.

1346



(a) Fluid properties based on wall temperature.



(b) Fluid properties based on stream temperature.

Figure 4. - Theoretical effect on heat transfer of temperature ratio and Mach number for gas properties at wall or stream temperature (reference 9).
 $Pr = 0.725$; $\omega = 0.75 = \phi$; $\beta = 0$; $Eu = 0$.

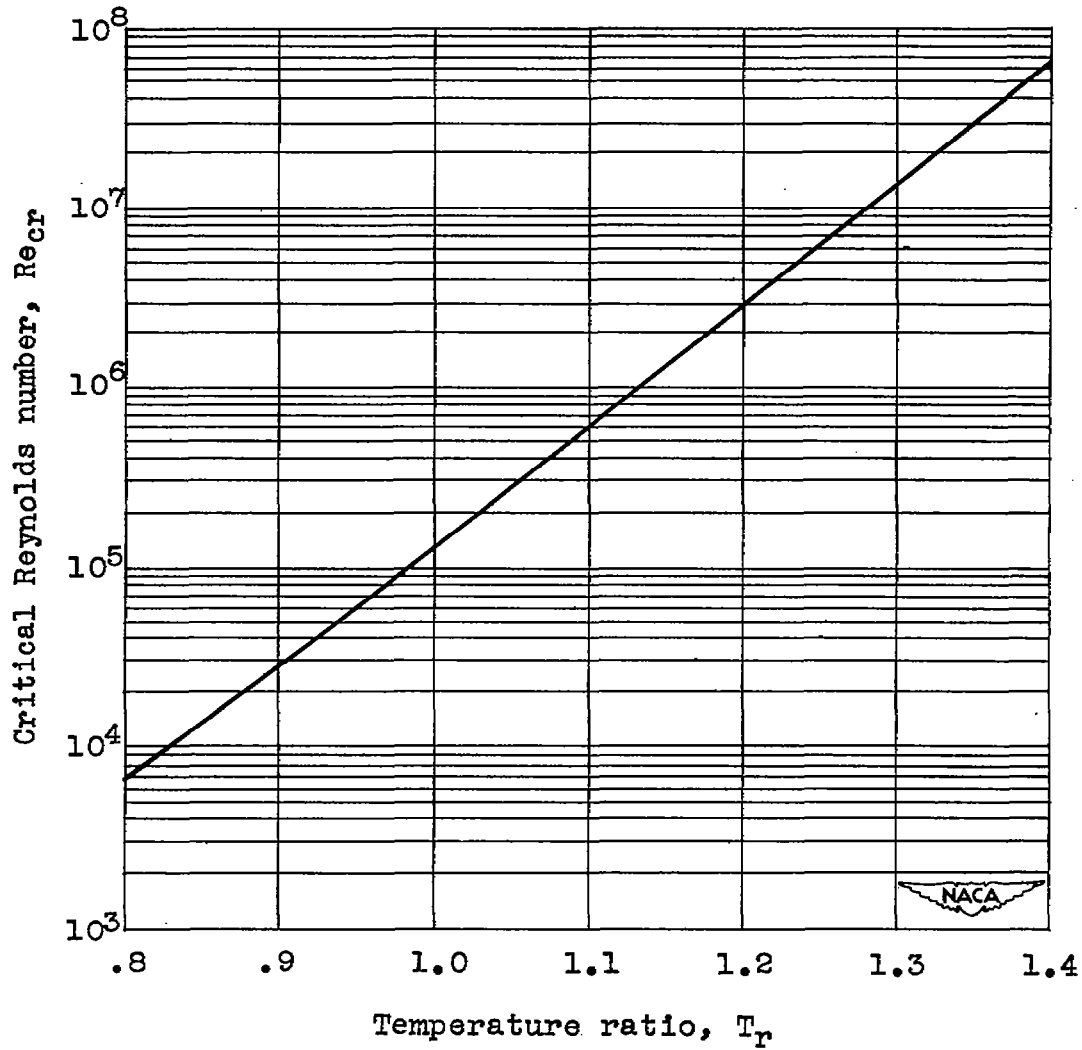


Figure 5. - Theoretical effect of temperature ratio on stability of laminar boundary layer (reference 18). $M = 0.7$; $\omega = 0.76$; $Eu = 0$; $Pr = 1.0$.

1346

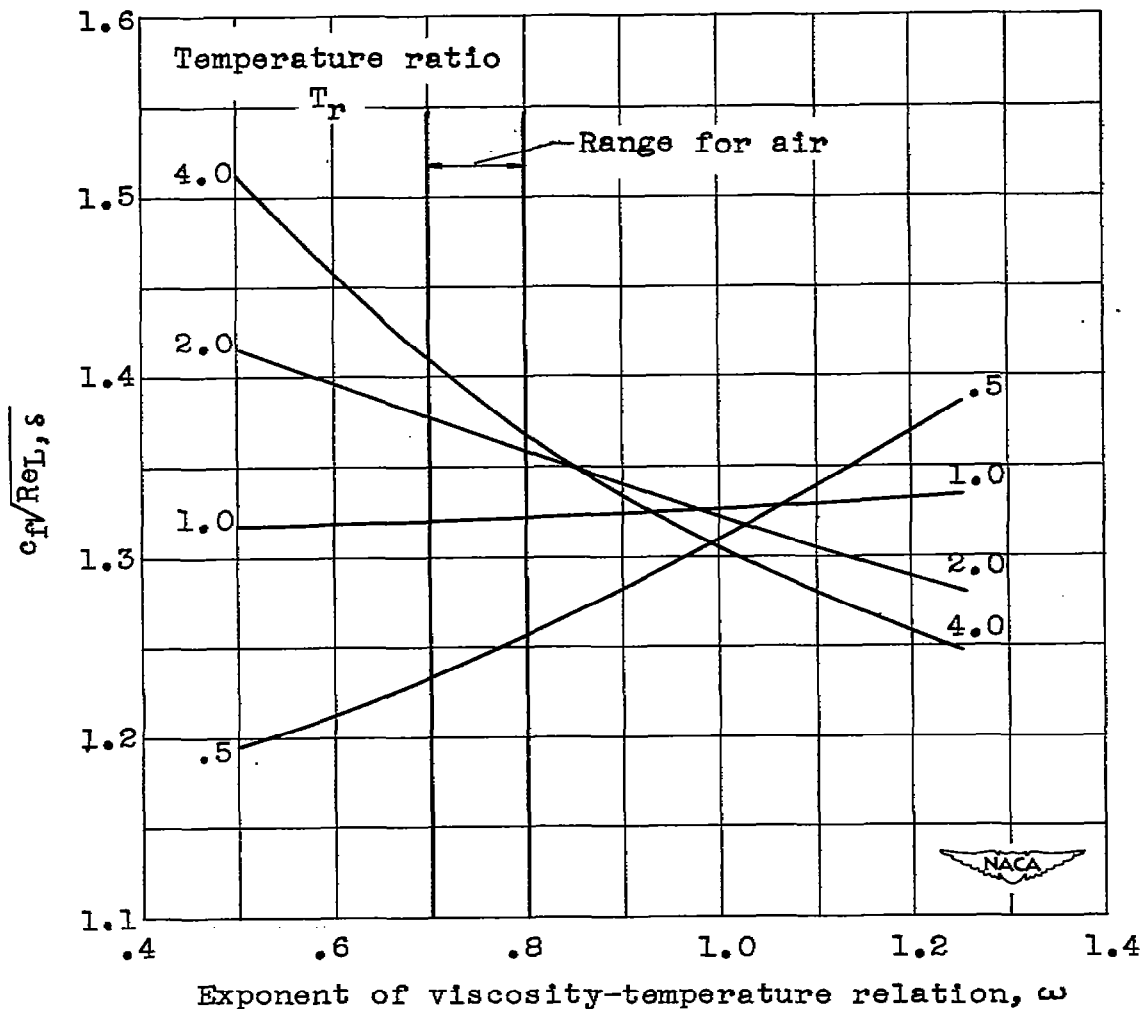


Figure 6. - Theoretical effect of ω on heat transfer with laminar boundary layer (reference 4). $M = 1.0$; $Pr = 0.725$; $\omega = \phi$; $\beta = 0$; $Eu = 0$; $\mu \propto T^\omega$;

$$Nu_{L,s} / \sqrt{Re_{L,s}} \propto c_f \sqrt{Re_{L,s}}$$

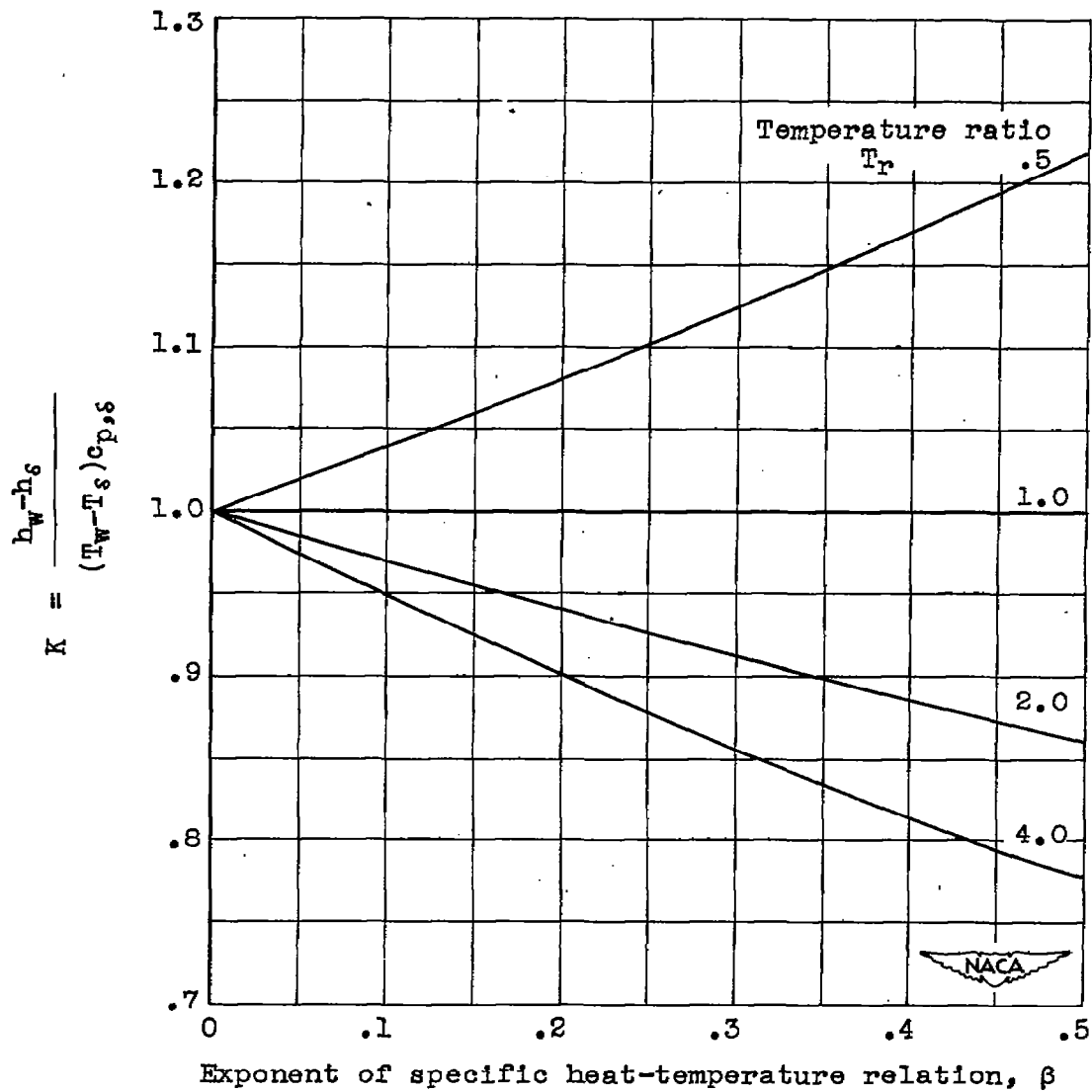


Figure 7. - Theoretical effect of β on heat transfer with laminar boundary layer (reference 4). $Pr = 0.725$;

$$Nu_{L,s} / \sqrt{Re_{L,s}} \propto \frac{h_w - h_s}{(T_w - T_s) c_{p,s}} ; \quad c_p / c_{p,w} = (T/T_w)^\beta .$$

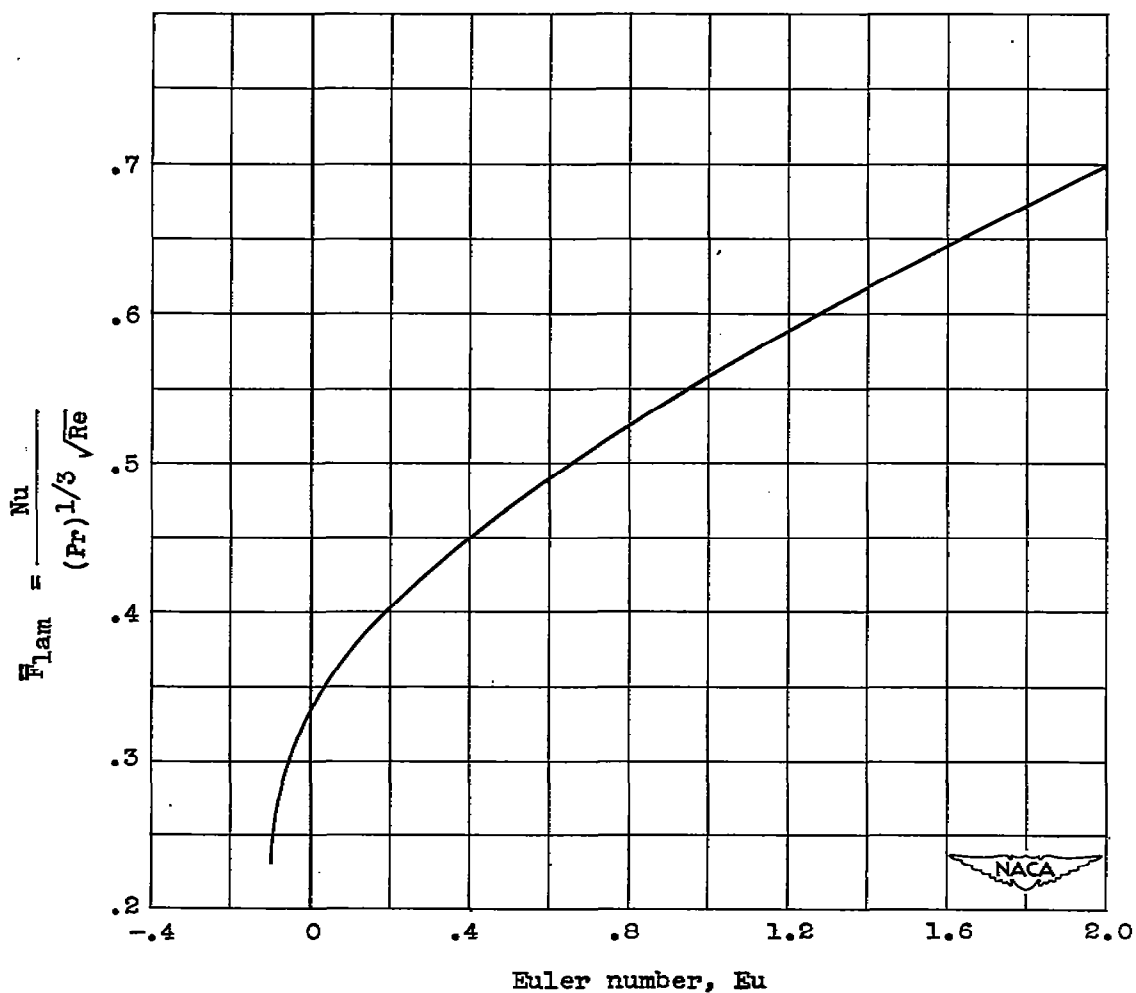


Figure 8. - Effect of Euler number on heat transfer with laminar boundary layer. $T_r \approx 1.0$; $M \approx 0$;

$$Eu = \frac{-dp/dx}{\rho_s U^2/x}$$

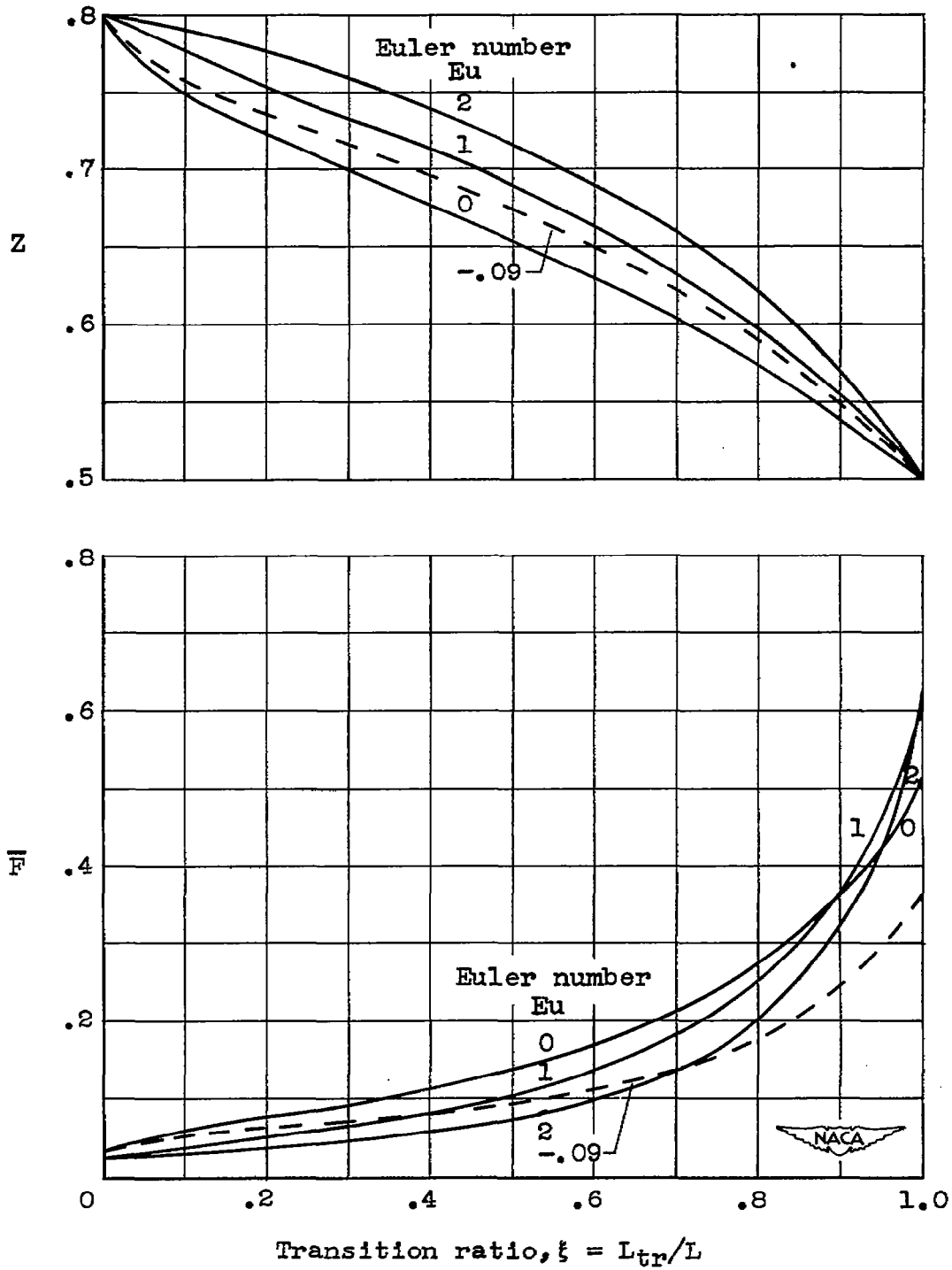


Figure 9. - Effect of transition and Euler number on correlation equation $Nu_p/(Pr)^{1/3} = \bar{F}(Re_p)Z$.

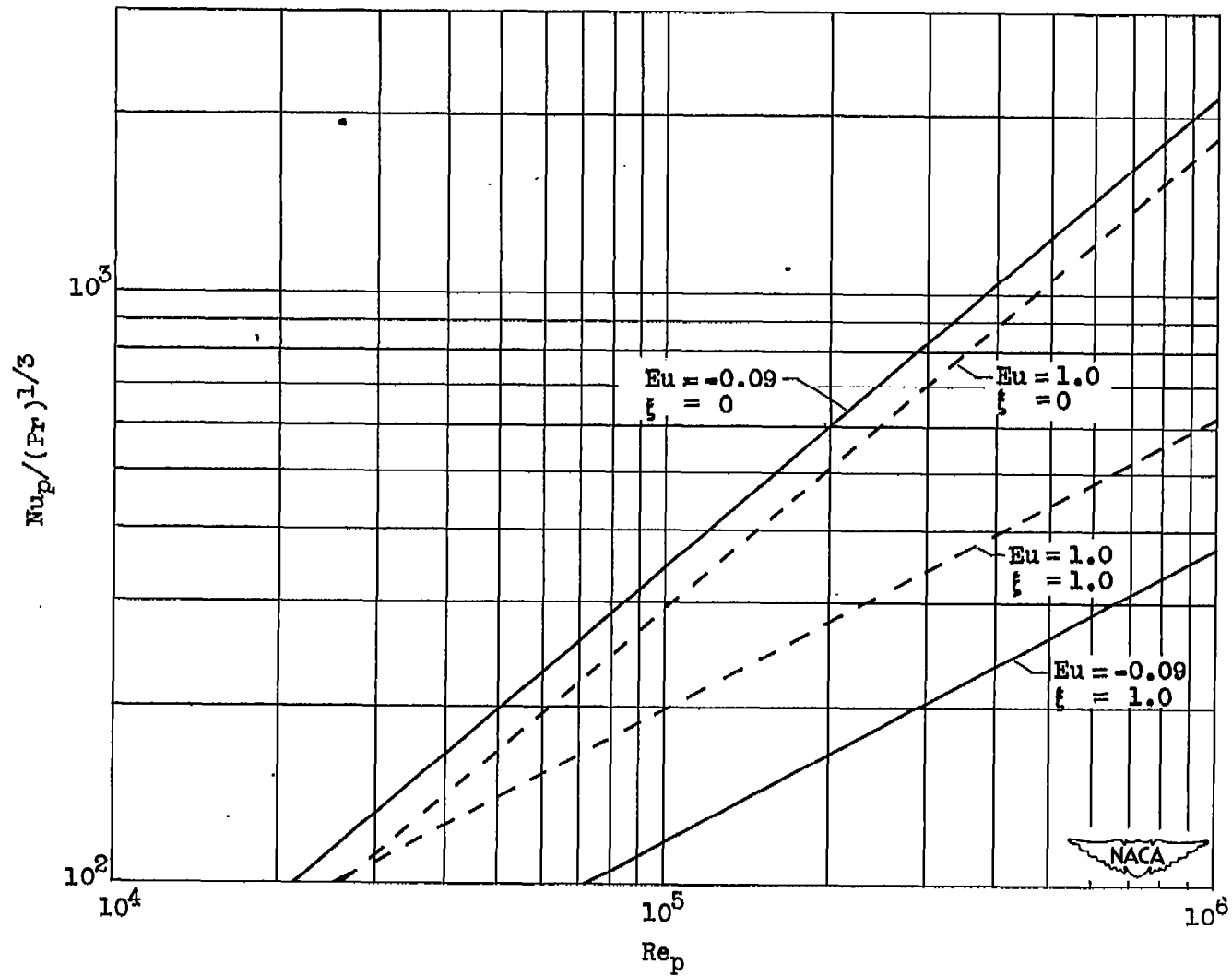


Figure 10. - Theoretical curves for heat transfer with Euler numbers of -0.09 and 1.0 with limiting values of transition ratio.

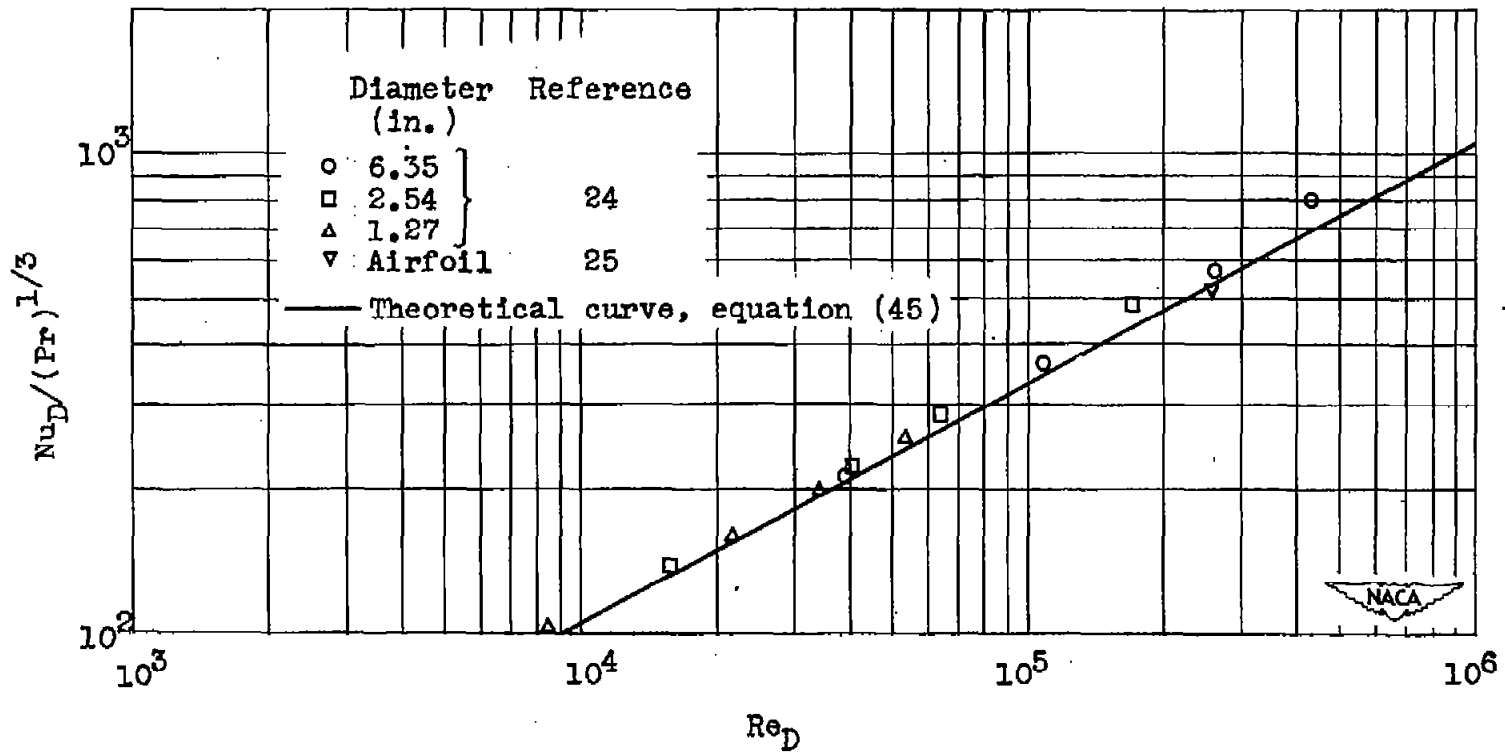


Figure 11. - Heat-transfer correlation at forward stagnation point. (Experimental data from references 24 and 25.)

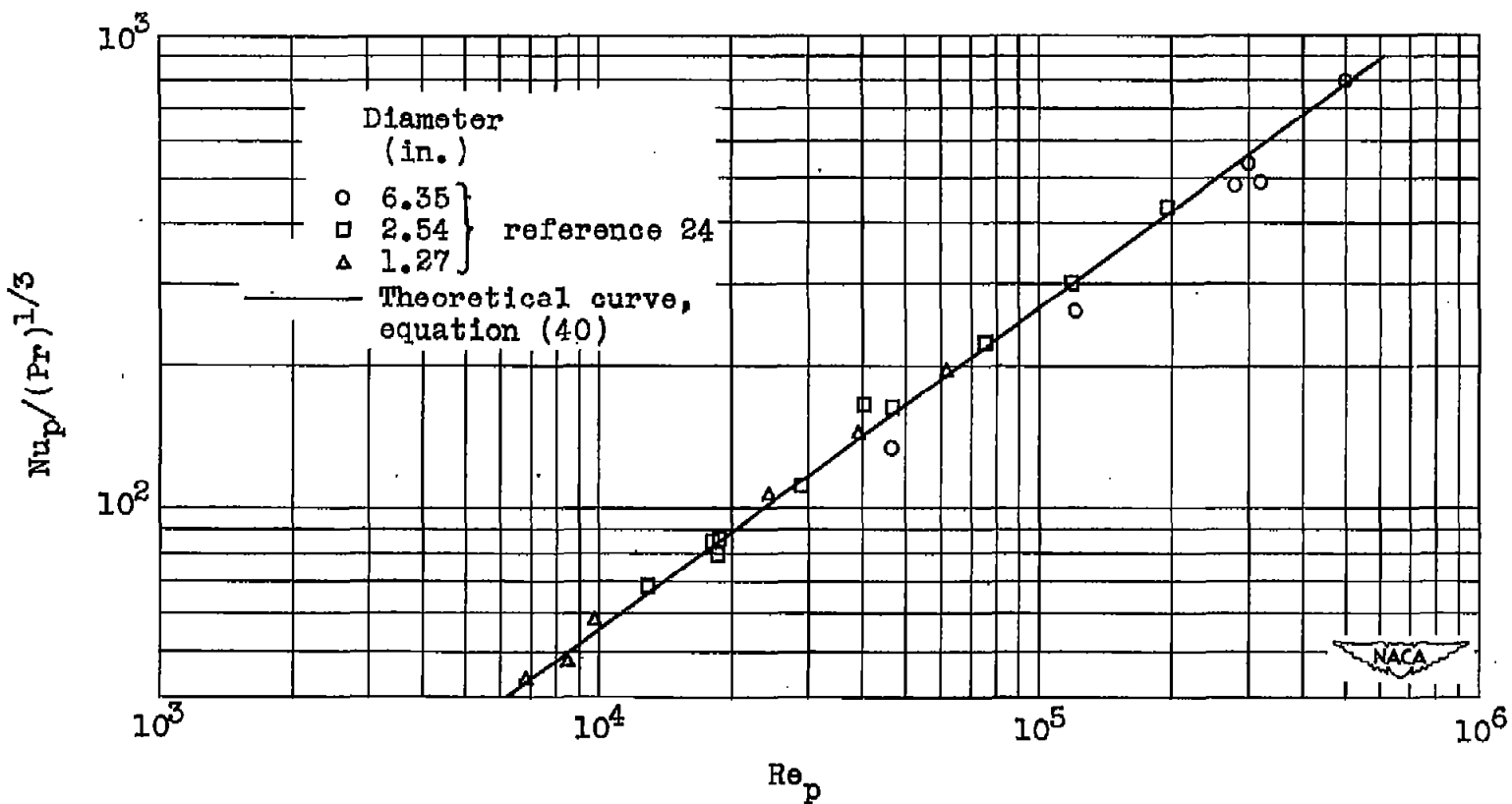


Figure 12. - Comparison of experimental data for average Nusselt number from cylinders with theoretical curve for $Eu = 0.55$ and $\xi = 0.455$ (data from reference 24).

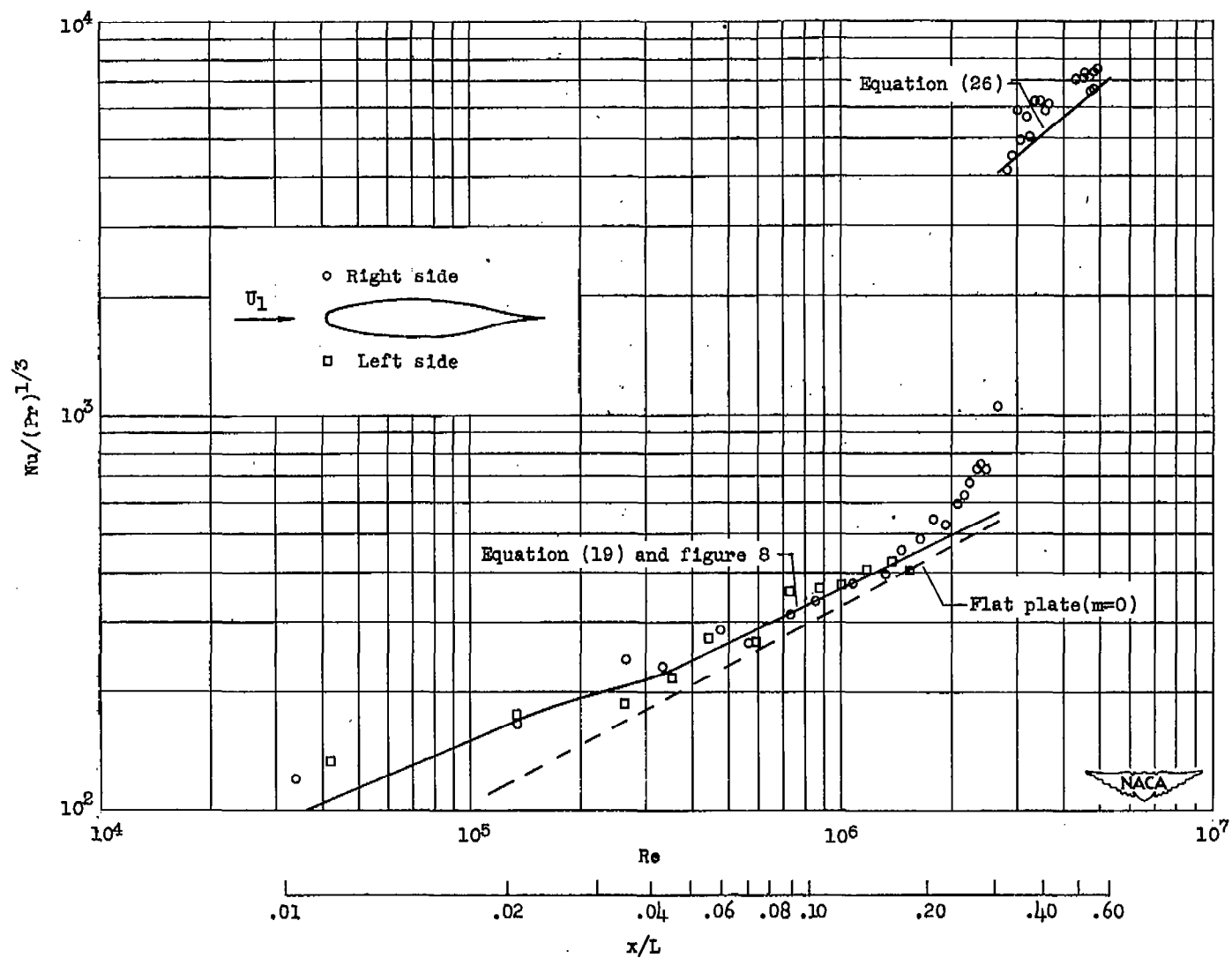


Figure 13. - Comparison of local heat-transfer obtained theoretically and from experiment of reference 25.

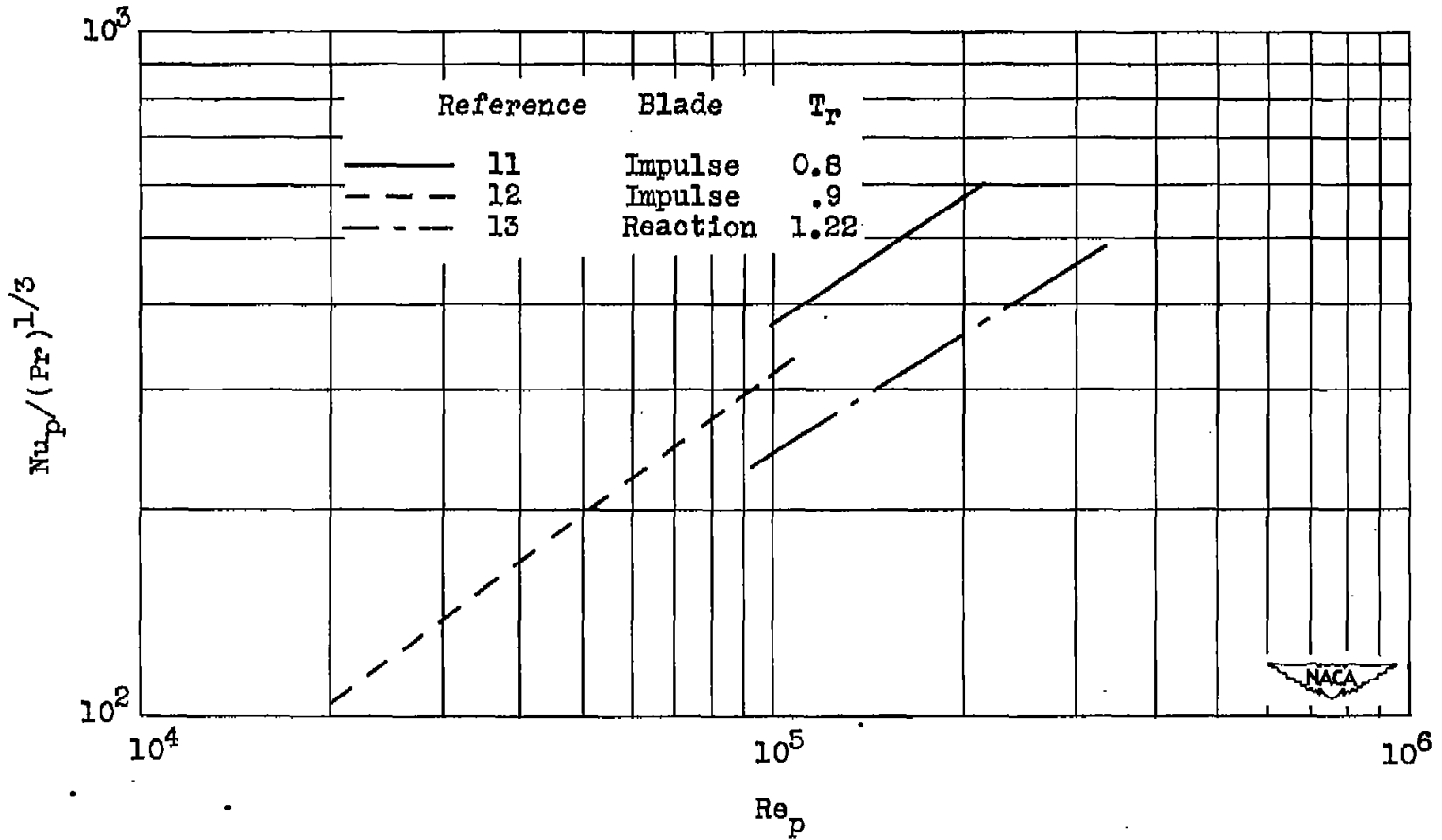


Figure 14. - Correlation of heat-transfer data around heated and cooled turbine blades.

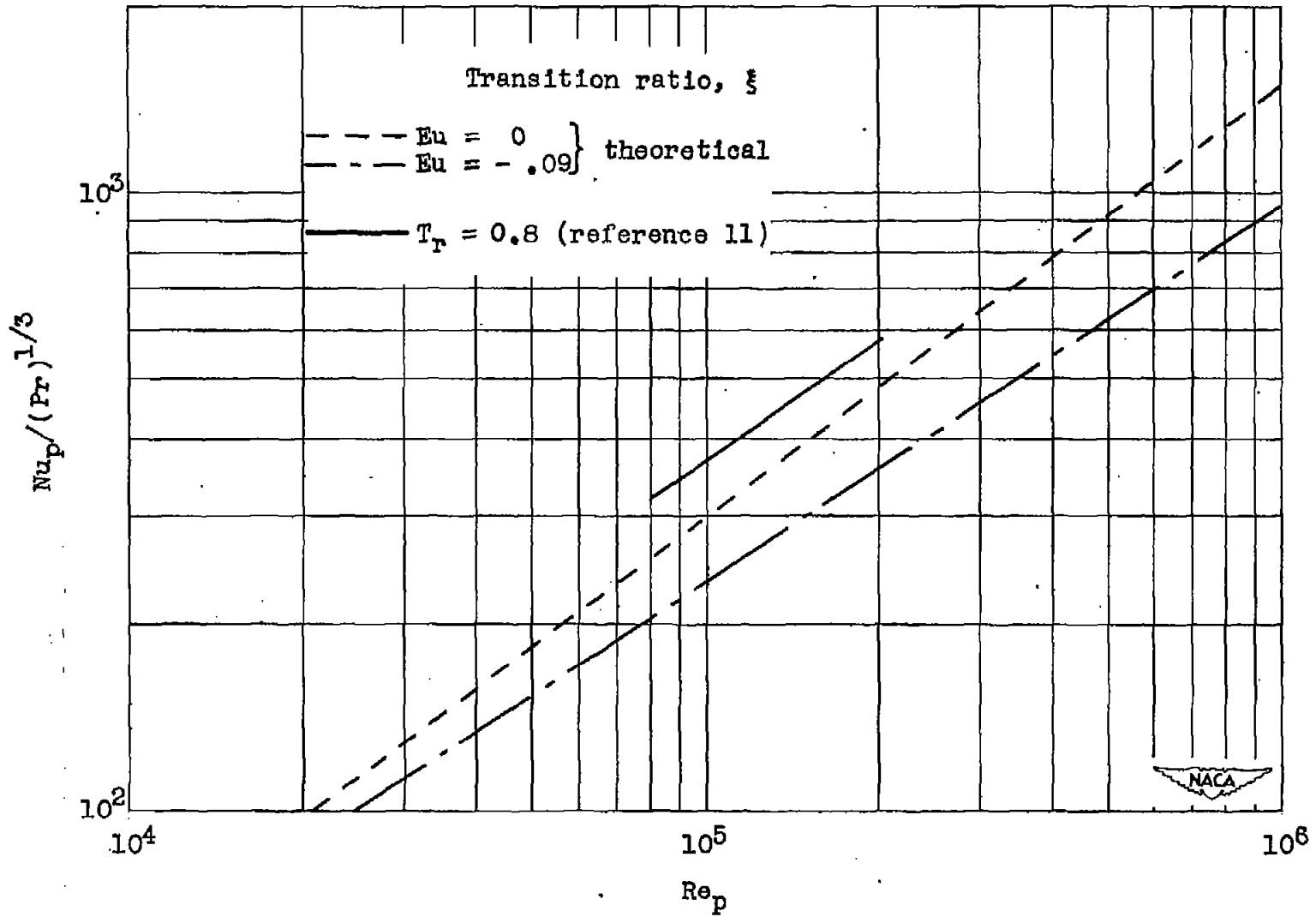


Figure 15. - Comparison of theory with experimental data of reference 11.
 Impulse blade; temperature ratio, 0.8.

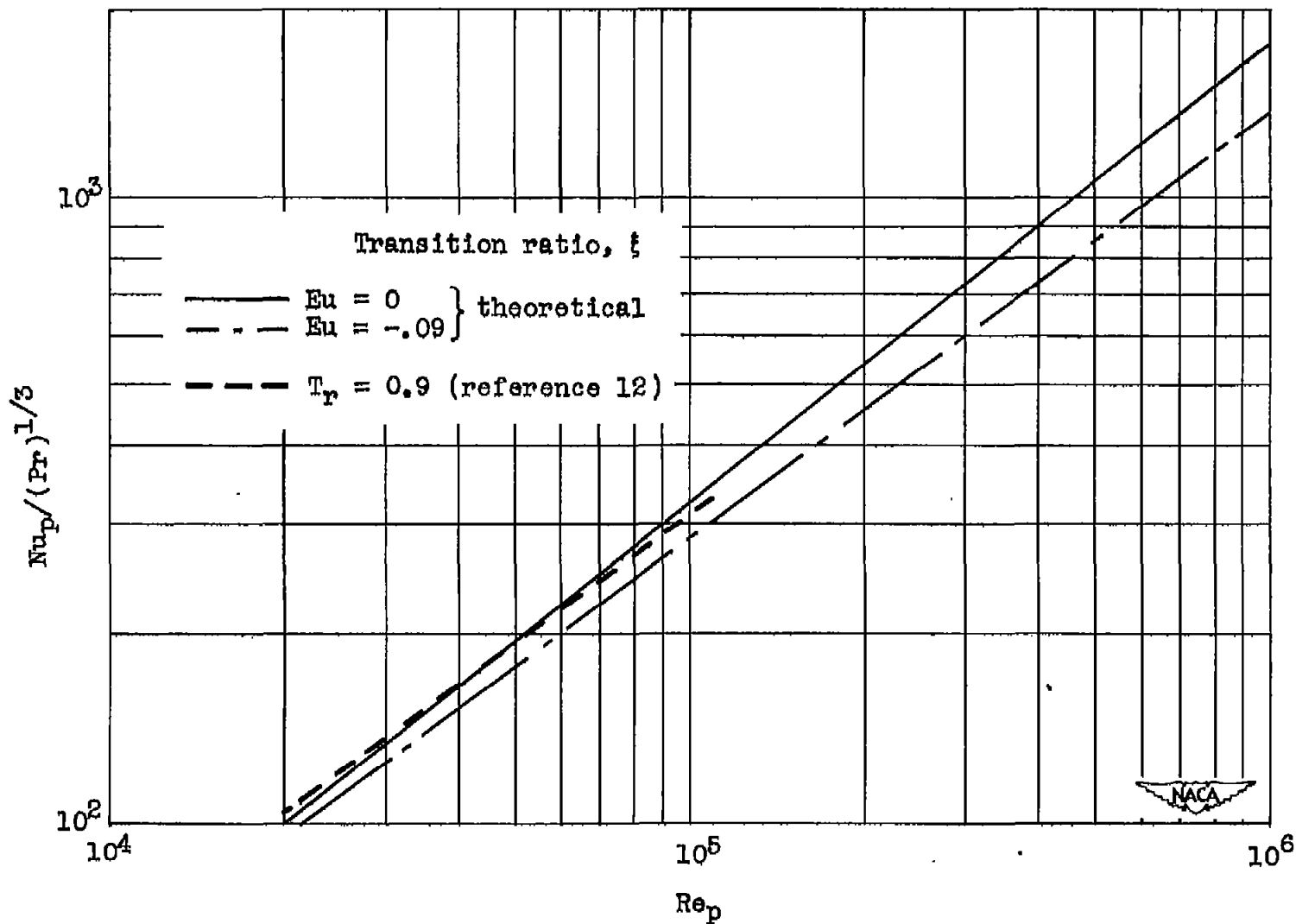


Figure 16. - Comparison of theory with experimental data of reference 12.
 Impulse blade; temperature ratio, 0.9.

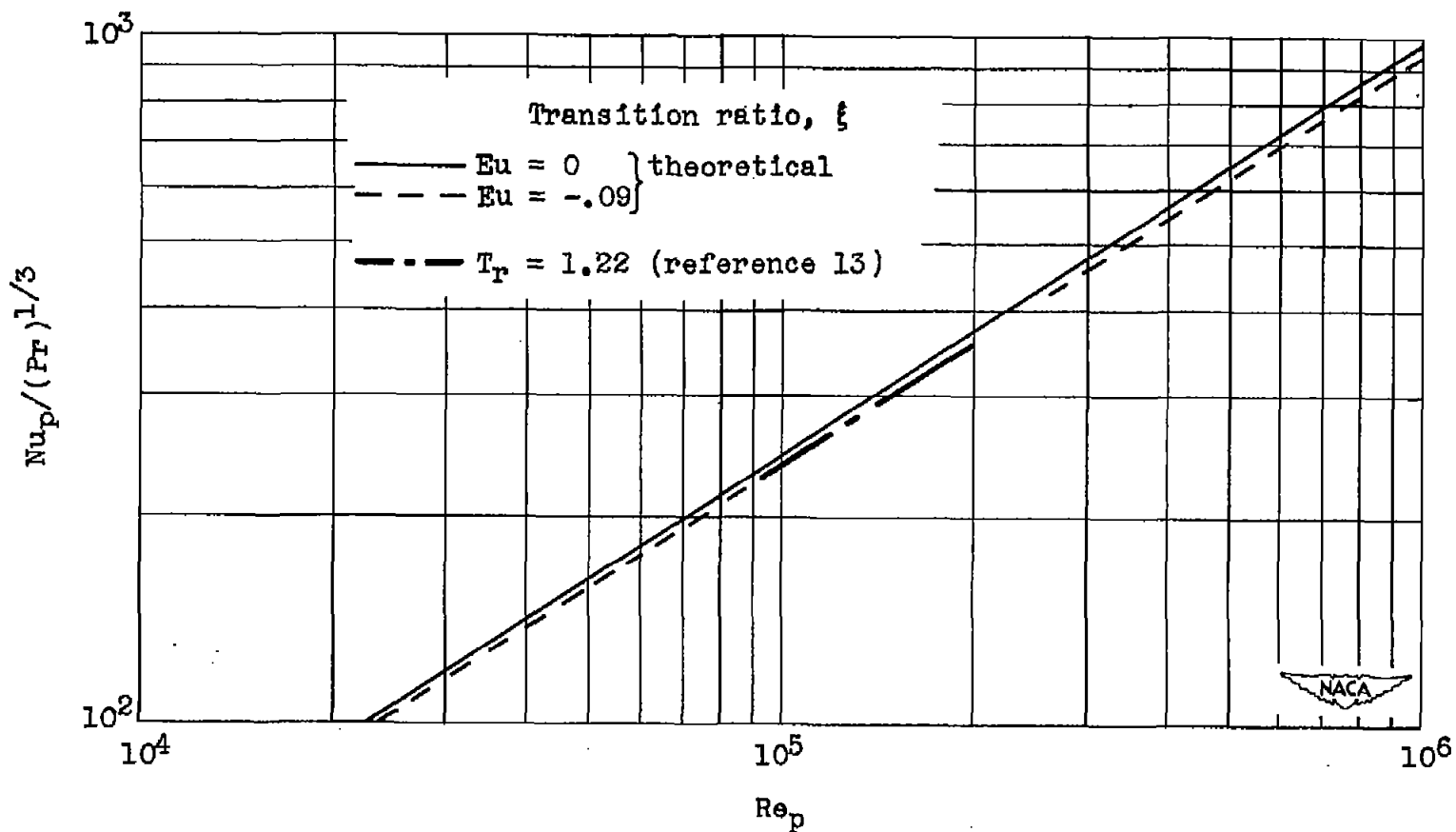


Figure 17. - Comparison of theory with experimental data of reference 13.
Reaction blade; temperature ratio, 1.22.

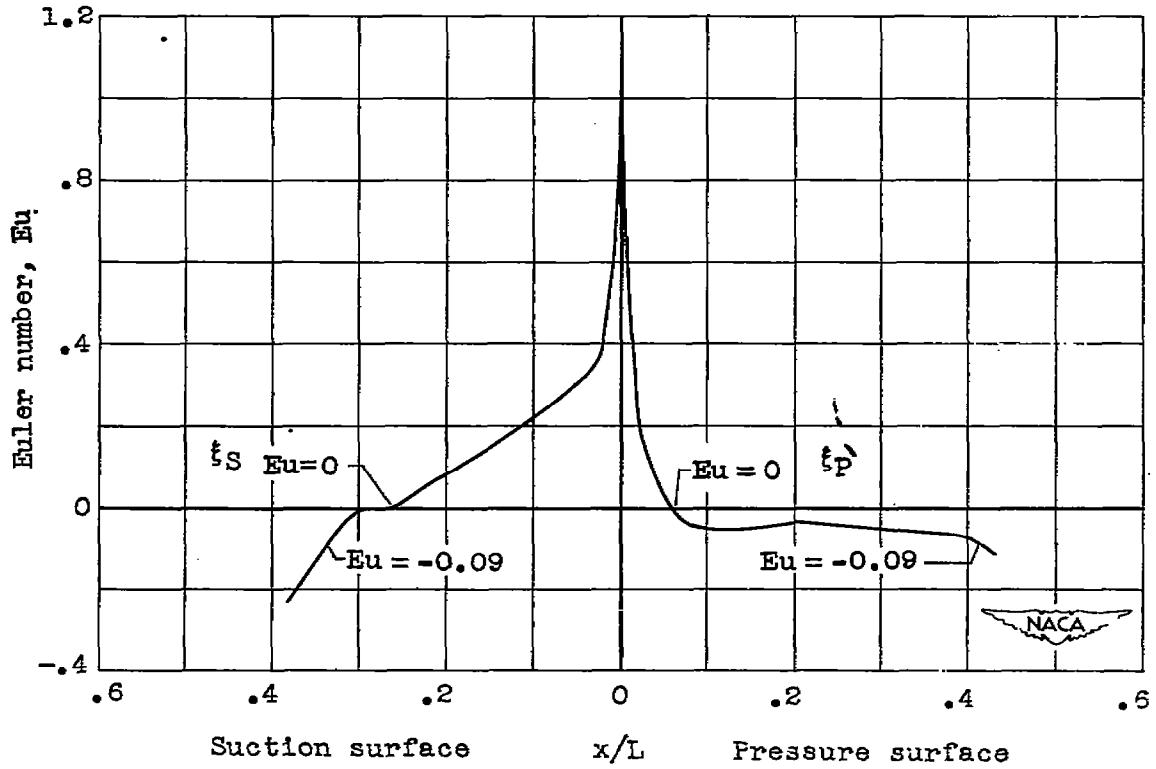


Figure 18. - Variation of local Euler number for reference 12.

NASA Technical Library



3 1176 01434 4973